SUPPLEMENTAL MATERIALS

Absence of the KhpA and KhpB (JAG/EloR) RNA-Binding Proteins Suppresses the Requirement for PBP2b by Overproduction of FtsA in *Streptococcus pneumoniae* D39

Jiaqi J. Zheng[1], Amilcar J. Perez[1], Ho-Ching Tiffany Tsui[1*], Orietta Massidda[2], and Malcolm E. Winkler[1]*

[1]Department of Biology, Indiana University Bloomington (IUB), Bloomington, IN 47405 USA [2]Dipartimento di Scienze Chirurgiche, Università di Cagliari, 09100 Cagliari, Italy

*Corresponding author:
Malcolm E. Winkler
Phone: 812-856-1318
E-mail: winklerm@indiana.edu

*Co-corresponding author
Ho-Ching Tiffany Tsui
Phone: 812-856-1781
E-mail: tttsui@indiana.edu

SUPPLEMENTAL TABLES

Table S1. *Streptococcus pneumoniae* strains and oligonucleotide primers used in this study

Table S2. Spontaneous suppressor mutations in D39 Δ*cps* Δ*pbp2b* strains identified by Illumina whole-genome or conventional sequencing

Table S3. mRNA-Seq results for a Δ*khpA* mutant

Table S4. Because of its size, **“Table S4**. RNAs pulled down by KhpA or KhpB in RIP-Seq experiments” is appended to the end of the Supplemental Materials.

SUPPLEMENTAL FIGURE LEGENDS.

Fig. S1. Model of PG biosynthesis in ovococcus bacteria, such as *S. pneumoniae*, and topology of proteins involved in peripheral PG synthesis.

Fig. S2. KhpA and KhpB are conserved in important Gram-positive pathogenic bacteria.

Fig. S3. Δ*khpA* reduces growth rate and cell size of encapsulated D39 and TIGR4 *Streptococcus pneumoniae* strains.

Fig. S4. The *mltG*(Y488D) Δ*khpA* double mutant grows slower than either *mltG*(Y488D) or Δ*khpA* single mutant.

Fig. S5. Δ*khpA* suppresses Δ*pbp2b*, Δ*mreCD*, Δ*rodZ,* Δ*rodA*, and Δ*gpsB* mutations in the D39 genetic background.

Fig. S6. Absence of growth and morphology defects of strains expressing KhpA-L-FLAG^3 or KhpB-L-FLAG^3 from their native chromosomal loci.

Fig. S7. Similar growth and cell morphology of the Δ*khpA* Δ*khpB* double and Δ*khpA* Δ*khpB* Δ*pbp2b* triple mutants.

Fig. S8. KhpA and KhpB co-localize at all stages of the bacterial cell cycle.

Fig. S9. Protein phosphorylation is reduced slightly in Δ*khpA*, Δ*khpA,* and Δ*khpA* Δ*khpB* mutants.

Fig. S10. Phosphoablative and phosphomimetic amino acid changes of KhpB at Thr89 (see Fig. 1B) does not affect growth and cell morphology.

Fig. S11. Amino acid changes in the KhpA(GXXG) motif destabilizes KhpA and results in a Δ*khpA* phenotype.

Fig. S12. RIP-qRT-PCR control confirms results and specificity of RIP-Seq experiments.

Fig. S13. FtsA is overproduced in the Δ*pbp2b sup6* strain.

Fig. S14. Relative cellular amount of FtsZ is increased by ≈1.9-fold by ectopic overexpression.

Fig. S15. Ectopic overexpression of *ftsA* does not change relative cellular FtsZ amount.

Fig. S16. FtsA overproduction partially contributed to the phenotypes of Δ*khpA* mutant.

Fig. S17. Linearity of signal intensity in Western blots versus protein amount in lysates.

Fig. 18. JBrowse profile illustrating enrichment of mRNA near the 5'-UTR and start codon of *ftsA* and mRNA of *sepF* by KhpA-L-FLAG^3 or KhpB-L-FLAG^3 pull down in RIP-Seq experiments compared to the wild-type (WT) control strain, which does not express a FLAG^3-tagged protein.

Fig. 19. Δ*khpA* and Δ*khpB* mutants are slightly more resistant to gentamicin, but have the same sensitivities to β-lactam antibiotics or tetracycline as the wild-type (WT) strain.

Fig. S20. The Δ*khpA* Δ*walK* double mutant grows slower than either Δ*walK* or Δ*khpA* single mutant.

Fig. S21. KhpB overproduction does not alter growth and cell morphology of D39-derived strains.

SUPPLEMENTAL REFERENCES

Table S4. RNAs pulled down by KhpA or KhpB in RIP-Seq experiments

Table S1. *Streptococcus pneumoniae* strains and oligonucleotide primers used in this study

Strains used in this study			
Strain number	Genotype (description)^{a}	Antibiotic resistance^{b}	Reference or source
IU1690	D39 *cps*$^{+}$	None	Lanie *et al*., 2007
IU1824^{c}	D39 *rpsL1* Δ*cps2A'-cps2H'* = D39 *rpsL1* Δ*cps*	Str^{R}	Lanie *et al*., 2007
IU1945	D39 Δ*cps2A'-cps2H'*= D39 Δ*cps*	None	Lanie *et al*., 2007
E217	D39 Δ*cps* Δ*walK*::P$_{c}$-*erm*	Erm^{R}	Wayne *et al*., 2010
K751	D39 Δ*cps* Δ*khpA*::P$_{c}$-[*kan-rpsL*$^{+}$] (IU1945 X fusion Δ*khpA*::P$_{c}$-[*kan-rpsL*$^{+}$])	Kan^{R}	This study
E751	D39 Δ*cps* Δ*khpA*::P$_{c}$-*erm* (IU1945 X fusion Δ*khpA*::P$_{c}$-erm)	Erm^{R}	This study
K761	D39 Δ*cps* Δ*khpB*::P$_{c}$-[*kan-rpsL*$^{+}$] (IU1945 X fusion Δ*khpB*::P$_{c}$-[*kan-rpsL*$^{+}$])	Kan^{R}	This study
IU4888	D39 Δ*cps* Δ*gpsB<>aad9*//Δ*bgaA*::*kan*-t1t2-P$_{fcsK}$-*gpsB*$^{+}$	Kan^{R} Spc^{R}	Land *et al*., 2013
IU4970	D39 Δ*cps* *mreC*-L-FLAG^{3}-P$_{c}$-*erm*	Erm^{R}	Land *et al*., 2011
IU5557	D39 Δ*cps* Δ*bgaA*::*kan*-t1t2-P$_{fcsK}$-*ftsZ*$^{+}$ (IU1945 transformed with fusion amplicon, Δ*bgaA*::*kan*-t1t2-P$_{fcsK}$-*ftsZ*$^{+}$)	Kan^{R}	This Study
IU5809	D39 Δ*cps* *spd_1366*-L-FLAG^{3}-P$_{c}$-*erm* (IU1945 X fusion *spd_1366*-L-FLAG^{3}-P$_{c}$-*erm*)	Erm^{R}	This study
IU6397	D39 *rpsL1* Δ*phoU2* Δ*bgaA*::*kan-T1T2*-P$_{ftsA}$-*phoU2*$^{+}$	Str^{R} Kan^{R}	Zheng *et al*., 2016
IU6741	D39 *rpsL1* Δ*pbp1a*	Str^{R} Kan^{S}	Tsui *et al*., 2016
IU7054	D39 Δ*cps* Δ*bgaA*::*kan-t1t2*-P$_{ftsA}$-RBS^{ftsA}-*ftsZ*$^{+}$ (IU1945 transformed with fusion amplicon, Δ*bgaA*::*kan*-t1t2-P$_{ftsA}$-RBS^{ftsA}-*ftsZ*$^{+}$)	Kan^{R}	This Study
IU7397	D39 Δ*cps* Δ*pbp2b<>aad9*//Δ*bgaA*::*kan*-t1t2-P$_{fcsK}$-*pbp2b*$^{+}$	Kan^{R} Spc^{R}	Tsui *et al*., 2014
IU7476	D39 Δ*cps* Δ*pbp2b<>aad9 sup1* (IU1945 X Δ*pbp2b<>aad9* from IU7397)	Spc^{R}	This study
IU7814	D39 Δ*cps* Δ*ftsZ*::*aad9*//*bgaA'*::*kan*-t1t2-P$_{ftsA}$-RBS^{ftsA}-*ftsZ*$^{+}$ (IU7054 transformed with fusion amplicon, Δ*ftsZ*::*aad9*)	Kan^{R} Spc^{R}	This Study
IU7915	D39 Δ*cps* *rpsL1* Δ*khpA*::P$_{c}$-[*kan-rpsL*$^{+}$] (IU1824 X Δ*khpA*::P$_{c}$-[*kan-rpsL*$^{+}$] from K751)	Kan^{R} Str^{S}	This study

IU7942	D39 Δ*cps rpsL1 khpA* (ΔA at K71) (IU7915 X *khpA* (ΔA at K71) from IU7476)	Kan^S Str^R	This study
IU8011	D39 Δ*cps rpsL1 khpA* (ΔA at K71) Δ*pbp2b<>aad9* (IU7942 X Δ*pbp2b<>aad9* from IU7397)	Kan^S Str^R Spc^R	This study
IU8122	D39 Δ*cps* Δ*bgaA*::*tet*-P$_{Zn}$-RBS^{ftsA}-*ftsZ*$^+$ (IU1945 X fusion Δ*bgaA*::*tet*-P$_{Zn}$-*ftsZ*$^+$)	Tet^R	This study
IU8872	D39 Δ*cps* Δ*bgaA*::*tet*-P$_{Zn}$-RBS^{mltG}-*mltG*$^+$	Tet^R	Tsui *et al*., 2016
IU9036	D39 Δ*cps rpsL1* Δ*khpA* (IU7915 X fusion Δ*khpA*)	Kan^S Str^R	This study
IU9600	D39 Δ*khpA*::P$_c$-*erm* (IU1690 X Δ*khpA*::P$_c$-*erm* from E751)	Erm^R	This study
IU9602	D39 Δ*cps khpA*-L-FLAG^3-P$_c$-*erm* (IU1945 X fusion *khpA*-L-FLAG^3-P$_c$-*erm*)	Erm^R	This study
IU9621	D39 Δ*cps rpsL1* Δ*khpA*//Δ*bgaA*::*kan*-t1t2-P$_{ftsA}$-*khpA*$^+$ (IU9036 X fusion Δ*bgaA*::*kan*-t1t2-P$_{ftsA}$-*khpA*$^+$)	Str^R Kan^R	This study
IU9697	D39 Δ*cps rpsL1 khpA*-L-FLAG^3 (IU7915 X fusion *khpA*-L-FLAG^3)	Str^R Kan^S	This study
IU9760	D39 Δ*cps rpsL1 mltG*(Y488D)	Str^R Kan^S	Tsui *et al*., 2016
IU9763	D39 Δ*cps rpsL1* Δ*khpA* Δ*pbp2b<>aad9* (IU9036 X Δ*pbp2b<>aad9* from IU7397)	Kan^S Str^R Spc^R	This study
IU9767	D39 Δ*cps rpsL1* P$_c$-[*kan-rpsL*$^+$]-*ftsA*$^+$	Kan^R Str^S	Mura *et al*., 2017
IU9935	D39 Δ*cps rpsL1 khpA* (G49A) (IU7915 X fusion *khpA* (G49A) amplicon)	Kan^S Str^R	This study
IU9937	D39 Δ*cps rpsL1 khpA* (G52A) (IU7915 X fusion *khpA* (G52A) amplicon)	Kan^S Str^R	This study
IU9939	D39 Δ*cps rpsL1 khpA*(G49A)-L-FLAG^3 (IU7915 X fusion *khpA*(G49A)-L-FLAG^3 amplicon)	Kan^S Str^R	This study
IU9941	D39 Δ*cps rpsL1 khpA*(G52A)-L-FLAG^3 (IU7915 X fusion *khpA*(G52A)-L-FLAG^3 amplicon)	Kan^S Str^R	This study
IU9977	D39 Δ*cps rpsL1 khpA* (G49A G52A) (IU7915 X fusion *khpA* (G49A G52A) amplicon)	Kan^S Str^R	This study
IU9979	D39 Δ*cps rpsL1 khpA*(G49A G52A)-L-FLAG^3 (IU7915 X fusion *khpA*(G49A G52A)-L-FLAG^3 amplicon)	Kan^S Str^R	This study
IU9990	D39 Δ*cps* Δ*bgaA*::*tet*-P$_{Zn}$-RBS^{ftsA}-*pbp2b*$^+$ (IU1945 X fusion Δ*bgaA*::*tet*-P$_{Zn}$-RBS^{ftsA}-*pbp2b*$^+$)	Tet^R	This study
IU10080	D39 Δ*cps rpsL1* Δ*khpA* Δ*walK*::P$_c$-*erm* (IU9036 X Δ*walK*::P$_c$-*erm* from E217)	Erm^R	This study

IU10091	D39 Δ*cps rpsL1 khpA* (R50D K51D) (IU7915 X fusion *khpA* (R50D K51D) amplicon)	Kan^S Str^R	This study
IU10092	D39 Δ*cps rpsL1 khpA* (R50D K51D)-L-FLAG^3 (IU7915 X fusion *khpA* (R50D K51D)-L-FLAG^3 amplicon)	Kan^S Str^R	This study
IU10230	D39 Δ*cps rpsL1* Δ*walK*::P$_c$-*erm* (IU1824 X Δ*walK*::P$_c$-*erm* from E217)	Erm^R	This study
IU10560	D39 Δ*cps rpsL1* Δ*khpB*::P$_c$-[*kan-rpsL*$^+$] (IU1824 X Δ*khpB*::P$_c$-[*kan-rpsL*$^+$] from K761)	Kan^R Str^S	This study
IU10562	D39 Δ*cps rpsL1* Δ*khpA* Δ*khpB*::P$_c$-[*kan-rpsL*$^+$] (IU9036 X Δ*khpB*::P$_c$-[*kan-rpsL*$^+$] from K761)	Kan^R Str^S	This study
IU10564	D39 Δ*cps rpsL1 khpA*-L-FLAG^3 Δ*khpB*::P$_c$-[*kan-rpsL*$^+$] (IU9697 X Δ*khpB*::P$_c$-[*kan-rpsL*$^+$] from K761)	Str^S Kan^R	This study
IU10592	D39 Δ*cps rpsL1* Δ*khpB* (IU10560 X fusion Δ*khpB*)	Kan^S Str^R	This study
IU10594	D39 Δ*cps rpsL1 khpB*-HA (IU10560 X fusion *khpB*-HA)	Kan^S Str^R	This study
IU10596	D39 Δ*cps rpsL1* Δ*khpA* Δ*khpB* (IU10562 X fusion Δ*khpB*)	Kan^S Str^R	This study
IU10602	D39 Δ*cps rpsL1 khpA*-L-F^3 *khpB*-HA (IU10564 X *khpB*-HA from IU10594)	Kan^S Str^R	This study
IU10624	D39 Δ*cps rpsL1* Δ*khpB* Δ*pbp2b<>aad9* (IU10592 X Δ*pbp2b<>aad9* from IU7397)	Kan^S Str^R Spc^R	This study
IU10626	D39 Δ*cps rpsL1* Δ*khpA* Δ*khpB* Δ*pbp2b<>aad9* (IU10596 X Δ*pbp2b<>aad9* from IU7397)	Kan^S Str^R Spc^R	This study
IU10651	D39 Δ*cps pbp1a*$^+$ *mltG*(Y488D) Δ*mreCD<>aad9*	Str^R Kan^S Spc^R	Tsui *et al*., 2016
IU10656	D39 Δ*cps pbp1a*$^+$ *mltG*(Y488D) Δ*rodZ(spd_2050)<>aad9*	Str^R Kan^S Spc^R	Tsui *et al*., 2016
IU10657	D39 Δ*cps rpsL1* Δ*khpA* Δ*mreCD<>aad9* (IU9036 X Δ*mreCD<>aad9* from IU10651)	Kan^S Str^R Spc^R	This study
IU10659	D39 Δ*cps rpsL1* Δ*khpA* Δ*rodZ<>aad9* (IU9036 X Δ*rodZ<>aad9* from IU10657)	Kan^S Str^R Spc^R	This study
IU10664	D39 Δ*cps khpB*-L-FLAG^3-P$_c$-*erm* (IU1945 X fusion *khpB*-L-FLAG^3-P$_c$-*erm*)	Erm^R	This study
IU10943	D39 Δ*cps rpsL1 mltG*(Y488D) Δ*rodA*::P$_c$-*erm*	Erm^R	Tsui *et al*., 2016
IU11246	D39 Δ*cps rpsL1* Δ*bgaA*::*tet*-P$_{Zn}$-RBS^{ftsA}-*pbp2b*$^+$ (IU1824 X Δ*bgaA*::*tet*-P$_{Zn}$-RBS^{ftsA}-*pbp2b*$^+$ from IU9990)	Tet^R	This study
IU11258	D39 Δ*cps rpsL1* Δ*bgaA*::*tet*-P$_{Zn}$-RBS^{ftsA}-*pbp2b*$^+$ Δ*pbp2b<>aad9* (IU11246 X Δ*pbp2b<>aad9* from IU7397)	Tet^R Spc^R	This study
IU11966	TIGR4 P1542	None	Tettelin *et al*., 2001

IU11970	D39 Δ*cps* Δ*pbp2b<>aad9 sup7 khpB* (ΔC at Q270) (IU1945 X Δ*pbp2b<>aad9* from IU7397)	Spc^{R}	This study
IU11971	D39 Δ*cps* Δ*pbp2b<>aad9 sup8 khpB* (ΩA at I102) (IU1945 X Δ*pbp2b<>aad9* from IU7397)	Spc^{R}	This study
IU11975	D39 Δ*cps* Δ*pbp2b<>aad9 sup9 khpB* (E143-stop) (IU1945 X Δ*pbp2b<>aad9* from IU7397)	Spc^{R}	This study
IU12013	D39 Δ*cps* Δ*pbp2b<>aad9 sup10 khpA* (M1-stop) (IU1945 X Δ*pbp2b<>aad9* from IU7397)	Spc^{R}	This study
IU12015	D39 Δ*cps* Δ*pbp2b<>aad9 sup6* ((Ω(*ddl'*-*ylmH'*)) (IU1945 X Δ*pbp2b<>aad9* from IU7397)	Spc^{R}	This study
IU12260	D39 Δ*cps rpsL1 mltG*(Y488D) Δ*khpA*::P$_{c}$-[*kan-rpsL*$^{+}$] (IU9760 X Δ*khpA*::P$_{c}$-[*kan-rpsL*$^{+}$] from K751)	Kan^{R} Str^{S}	This study
IU12286	D39 Δ*cps rpsL1* Δ*bgaA*::*tet*-P$_{Zn}$-RBS^{ftsA}-*ftsZ*$^{+}$ (IU1824 X Δ*bgaA*::*tet*-P$_{Zn}$-*ftsZ* from 8122)	Tet^{R}	This study
IU12288	D39 Δ*cps rpsL1 mltG*(Y488D) Δ*khpA* (IU12260 X fusion Δ*khpA*)	Kan^{S} Str^{R}	This study
IU12310	D39 Δ*cps rpsL1* Δ*bgaA*::*tet*-P$_{Zn}$-RBS^{ftsA}-*ftsA*$^{+}$	Str^{R} Tet^{R}	Mura *et al.*, 2017
IU12323	D39 Δ*cps* Δ*bgaA*::*tet*-P$_{Zn}$-RBS^{ftsA}-*ftsA*$^{+}$ Δ*ftsA*::*aad9*	Tet^{R} Spc^{R}	Mura *et al.*, 2017
IU12332	D39 Δ*cps rpsL1* Δ*pbp1a* Δ*cozE*::Pc-*erm* (IU6741 X fusion Δ*cozE*::Pc-*erm*)	Kan^{S} Str^{R} Erm^{R}	This study
IU12707	D39 Δ*cps rpsL1 ftsA*$^{+}$ Δ*pbp2b<>aad9* //Δ*bgaA*::*tet*-P$_{Zn}$-RBS^{ftsA}-*ftsA*$^{+}$ (IU12310 X Δ*pbp2b<>aad9* from IU7397)	Tet^{R} Spc^{R}	This study
IU12718	Δ*bgaA*::*kan*-t1t2-P$_{ftsA}$-*ftsA*$^{+}$ (IU1824 X fusion Δ*bgaA*::*kan*-t1t2-P$_{ftsA}$-*ftsA*$^{+}$)	Kan^{R}	This study
IU12744	D39 Δ*cps rpsL1 khpB* (T89A) (IU10560 X fusion *khpB* (T89A))	Kan^{S} Str^{R}	This study
IU12788	D39 Δ*cps rpsL1* Δ*bgaA*::*kan*-P$_{Zn}$-RBS^{ftsA}-*khpA*$^{+}$ (IU1824 X fusion Δ*bgaA*::*kan*-P$_{Zn}$-RBS^{ftsA}-*khpA*$^{+}$)	Kan^{R}	This study
IU12883	D39 Δ*cps rpsL1* Δ*khpA gpsB<>aad9* (IU9036 X Δ*gpsB<>aad9* from IU4888)	Kan^{S} Str^{R} Spc^{R}	This study
IU12887	D39 Δ*cps rpsL1* Δ*bgaA*::*tet*-P$_{Zn}$-RBS^{ftsA}-*ftsA*$^{+}$ Δ*mreCD<>aad9* (IU12310 X Δ*mreCD<>aad9* from IU10651)	Tet^{R} Spc^{R}	This study
IU12901	D39 Δ*cps rpsL1* Δ*bgaA*::*tet*-P$_{Zn}$-RBS^{ftsA}-*ftsA*$^{+}$ Δ*ftsA*::*aad9* (IU12310 X Δ*ftsA*::*aad9* from IU12323)	Str^{R} Tet^{R} Spc^{R}	This study
IU12927	D39 Δ*cps rpsL1* Δ*khpA* Δ*bgaA*::*tet*-P$_{Zn}$-RBS^{ftsA}-*ftsA*$^{+}$ (IU9036 X Δ*bgaA*::*tet*-P$_{Zn}$-RBS^{ftsA}-*ftsA*$^{+}$ from IU12310)	Str^{R} Kan^{S} Tet^{R}	This study

IU12929	D39 Δ*cps rpsL1* Δ*khpA* Δ*pbp2b*<>P$_c$-*erm* (IU9036 X fusion Δ*pbp2b*<>P$_c$-*erm*)	Str^R Kan^S Erm^R	This study
IU12959	D39 Δ*cps rpsL1* Δ*khpA* Δ*bgaA*::*tet*-P$_{Zn}$-RBS^{ftsA}-*ftsA*$^+$ Δ*ftsA*::*aad9* (IU12927 X Δ*ftsA*::*aad9* from IU12323)	Str^R Kan^S Tet^R Spc^R	This study
IU12973	D39 Δ*cps rpsL1* Δ*khpB* Δ*mreCD*<>*aad9* (IU10592 X Δ*mreCD*<>*aad9* from IU10651)	Kan^S Str^R Spc^R	This study
IU12975	D39 Δ*cps rpsL1* Δ*khpB* Δ*rodZ*<>*aad9* (IU10592 X Δ*rodZ*<>*aad9* from IU10657)	Kan^S Str^R Spc^R	This study
IU12977	D39 Δ*cps rpsL1* Δ*khpB gpsB*<>*aad9* (IU10592 X Δ*gpsB*<>*aad9* from IU4888)	Kan^S Str^R Spc^R	This study
IU12979	D39 Δ*cps rpsL1* Δ*khpB* ∆*rodA*::P$_c$-*erm* (IU10592 X ∆*rodA*::P$_c$-*erm* from IU10943)	Kan^S Str^R Erm^R	This study
IU13201	D39 Δ*cps rpsL1* Δ*bgaA*::*kan*-t1t2-P$_{ftsA}$-*ftsA*$^+$ Δ*ftsA*::*aad9* (IU12901 X Δ*bgaA*::*kan*-t1t2-P$_{ftsA}$-*ftsA*$^+$ from IU12718)	Str^R Kan^R Spc^R	This study
IU13204	D39 Δ*cps rpsL1* Δ*bgaA*::*kan*-t1t2-P$_{ftsA}$-*ftsA*$^+$ Δ*ftsA*::*aad9* Δ*khpA* (IU12959 X Δ*bgaA*::*kan*-t1t2-P$_{ftsA}$-*ftsA*$^+$ from IU12718)	Str^R Kan^R Spc^R	This study
IU13436	D39 Δ*cps rpsL1* Δ*khpA* ∆*rodA*::P$_c$-*erm* (IU9036 X ∆*rodA*::P$_c$-*erm* from IU10943)	Kan^S Str^R Erm^R	This study
IU13471	D39 Δ*cps rpsL1* Δ*bgaA*::*tet*-P$_{Zn}$-RBS^{ftsA}-*ftsA*$^+$ ∆*rodA*::P$_c$-*erm* (IU12310 X ∆*rodA*::P$_c$-*erm* from IU10943)	Tet^R Erm^R	This study
IU13479	D39 Δ*khpA*::Pc-*erm* Δ*pbp2b*<>*aad9* (IU9600 X Δ*pbp2b*<>*aad9* from IU7397)	Erm^R Spc^R	This study
IU13483	TIGR4 Δ*khpA*::Pc-*erm* (IU11966 X Δ*khpA*::P$_c$-*erm* from E751)	Erm^R	This study
IU13639	D39 Δ*cps rpsL1* Δ*khpA* P$_c$-[*kan-rpsL*$^+$]-*ftsA*$^+$ (IU9036 X P$_c$-[*kan-rpsL*$^+$]-*ftsA*$^+$ from IU9767)	Kan^R Str^S	This study
IU13641	D39 Δ*cps rpsL1 ftsA*(ΔUTR) (IU9767 X *ftsA*(ΔUTR) fusion amplicon)	Str^R Kan^S	This study
IU13672	D39 Δ*cps rpsL1* Δ*khpA ftsA*(ΔUTR) (IU13639 X *ftsA*(ΔUTR) from IU13641)	Str^R Kan^S	This study
IU13851	D39 Δ*cps rpsL1* Δ*khpB* P$_c$-[*kan-rpsL*$^+$]-*ftsA*$^+$ (IU10592 X P$_c$-[*kan-rpsL*$^+$]-*ftsA*$^+$ from IU9767)	Kan^R Str^S	This study
IU13853	D39 Δ*cps rpsL1* Δ*khpA* Δ*khpB* P$_c$-[*kan-rpsL*$^+$]-*ftsA*$^+$ (IU10596 X P$_c$-[*kan-rpsL*$^+$]-*ftsA*$^+$ from IU9767)	Kan^R Str^S	This study
IU13881	D39 Δ*cps rpsL1 khpB* (T89D) (IU10560 X fusion *khpB* (T89D))	Kan^S Str^R	This study
IU13883	D39 Δ*cps rpsL1 khpB* (T89E) (IU10560 X fusion *khpB* (T89E))	Kan^S Str^R	This study
IU13885	D39 Δ*cps rpsL1 khpB* (T89A) (IU10560 X *khpB* (T89A) from IU12744)	Kan^S Str^R	This study

IU13887	D39 Δ*cps rpsL1 khpB* (T89D) (IU10560 X fusion *khpB* (T89D))	Kan^{S} Str^{R}	This study
IU13889	D39 Δ*cps rpsL1 khpB* (T89E) (IU10560 X fusion *khpB* (T89E))	Kan^{S} Str^{R}	This study
IU13891	D39 Δ*cps rpsL1* Δ*khpB ftsA*(ΔUTR) (IU13851 X *ftsA*(ΔUTR) from IU13641)	Str^{R} Kan^{S}	This study
IU13893	D39 Δ*cps rpsL1* Δ*khpA* Δ*khpB ftsA*(ΔUTR) (IU13853 X *ftsA*(ΔUTR) from IU13641)	Str^{R} Kan^{S}	This study
IU14024	D39 Δ*cps rpsL1* Δ*bgaA*::*kan*-P$_{Zn}$-RBS^{ftsA}-*khpB*$^{+}$ (IU1824 X fusion Δ*bgaA*::*kan*-P$_{Zn}$-RBS^{ftsA}-*khpB*$^{+}$)	Kan^{R}	This study
IU14026	D39 Δ*cps rpsL1* Δ*bgaA*::*kan*-P$_{Zn}$-RBS^{ftsA}-*khpA*$^{+}$-*khpB*$^{+}$ (IU1824 X fusion Δ*bgaA*::*kan*-P$_{Zn}$-RBS^{ftsA}-*khpA*$^{+}$-*khpB*$^{+}$)	Kan^{R}	This study
Primers used to constructed strains			
Primer	Sequence (5’ to 3’)	Template^{d}	Amplicon Product
For construction of K751 (Δ*khpA*::P$_{c}$-[*kan-rpsL*$^{+}$])			
P1505	GGGGCATCAATGCCATAAGTGTACTCAAAG	D39	5’ flanking fragment with 12 bp of 5’ *khpA*
P1507	CATTATCCATTAAAAATCAAACGGATCCTACGCAATAATGAGATTTTCAATCGTATCC		
Kan rpsL forward	TAGGATCCGTTTGATTTTTAATGGATAATG	P$_{c}$-[*kan-rpsL*$^{+}$] cassette^{e}	P$_{c}$-[*kan-rpsL*$^{+}$]
Kan rpsL reverse	GGGCCCCTTTCCTTATGCTTTTG		
P1508	CAAAAGCATAAGGAAAGGGGCCCATTGTCTACTCTGTCCCAACTGAATACAAA	D39	3’ flanking fragment with 6 bp of 3’ *khpA*
P1506	GTCATGAATCGGACTCCTACCTGTGTTCGG		
For construction of K761 (Δ*khpB*::P$_{c}$-[*kan-rpsL*$^{+}$])			
P1539	AGTCGAAACCTTGGGATACGCAGAGATGGA	D39	5’ flanking fragment with 60 bp of 5’ *khpB*
P1542	AAACGTCCAAAAGCATAAGGAAAGGGGCCCGTGACTAGTTACTCTGAAGGTGATGAGCCA		
Kan rpsL forward	TAGGATCCGTTTGATTTTTAATGGATAATG	P$_{c}$-[*kan-rpsL*$^{+}$] cassette^{e}	P$_{c}$-[*kan-rpsL*$^{+}$]
Kan rpsL reverse	GGGCCCCTTTCCTTATGCTTTTG		
P1541	CATTATCCATTAAAAATCAAACGGATCCTATAATTCTTTCAATCCTTTCTGGATTGCTTC	D39	3’ flanking fragment with 60 bp of 3’ *khpB*
P1540	ACCGCTGCACCAATTTGGAATTTGTAGTTA		

For construction of E751 (Δ*khpA*:: P$_{c}$-*erm*)			
P1505	GGGGCATCAATGCCATAAGTGTACTCAAAG	D39	5’ flanking fragment with 12 bp of 5’ *khpA*
P1507	CATTATCCATTAAAAATCAAACGGATCCTACGCAATAATGAGATTTTCAATCGTATCC		
Kan rpsL forward	TAGGATCCGTTTGATTTTTAATGGATAATG	P$_{c}$-*erm* cassette^{e}	P$_{c}$-*erm*
Kan rpsL reverse	GGGCCCCTTTCCTTATGCTTTTG		
P1508	CAAAAGCATAAGGAAAGGGGCCCATTGTCTACTCTGTCCCAACTGAATACAAA	D39	3’ flanking fragment with 6 bp of 3’ *khpA*
P1506	GTCATGAATCGGACTCCTACCTGTGTTCGG		
For construction of IU5557 (Δ*bgaA*::*kan*-t1t2-P$_{fcsK}$-*ftsZ*$^{+}$)			
TT657	CGCCCCAAGTTCATCACCAATGACATCAAC	IU4888	Δ*bgaA*-P$_{c}$-*kan*-t1t2-P$_{fcsk}$
TT201	CAGCTGTATCAAATGAAAATGTCATTTTTCTTCTCTCTTCGTCCTTGATTAACTT		
TT202	ATCAAGGACGAAGAGAGAAGAAAAATGACATTTTCATTTGATACAGCTGCTG	D39	*ftsZ*$^{+}$
TT203	ACTGGTTTATGAGAAAGTAAGTTCTTTTATTAACGATTTTTGAAAAATGGAGGTGTATC		
TT396	CCTCCATTTTTCAAAAATCGTTAGAAGAACTTACTTTCTCATAAACCAGTTGCTG	D39	*bgaA’* 3’ flanking
CS121	GCTTTCTTGAGGCAATTCACTTGGTGC		
For construction of IU5809 (*spd_1366*-L-FLAG^{3}-P$_{c}$-*erm*)			
P594	AAGGGAGATGACTTGCACTTGCCTGACAGT	D39	5’ flanking fragment
DM215	CAGCGGAGCCAGCGGAACCCTTCTTCTTTTTTAAATGGTGCAGGGCTTCTC		
DM214	GAAGCCCTGCACCATTTAAAAAAGAAGAAGGGTTCCGCTGGCTCCGCTGCTG	IU4970	L-F^{3}- P$_{c}$-*erm*
DM212	CATTACAAAAAATATAAAACTCTAAATTTCCTCCCGTTAAATAATAGATAAC		
DM213	CTATTATTTAACGGGAGGAAATTTAGAGTTTTATATTTTTTGTAATGTTAAT	D39	3’ flanking fragment
P595	ACTGGCAAGCGTGCTCGTGTATATTTGGCT		
For construction of IU7054 (Δ*bgaA*::*kan*-t1t2-P$_{ftsA}$-RBS^{ftsA}-*ftsZ*$^{+}$)			
P146	TGGCCATTCATCGCTGGTCGTGCTGAAAT	IU6397	Δ*bgaA*::*kan*-t1t2-P$_{ftsA}$
TT393	CAGCTGTATCAAATGAAAATGTCATTACATCGCTTCCTCTCTATCTTCCAAGT		
TT394	GGAAGATAGAGAGGAAGCGATGTAATGACATTTTCATTTGATACAGCTGCTG	IU5557	3’ flanking containing *ftsZ*$^{+}$-*bgaA*’
CS121	GCTTTCTTGAGGCAATTCACTTGGTGC		
For construction of IU7814 (Δ*ftsZ*::*aad9*)			
AL366	GGCATGATGGGGGTTCGCCTTGAAATGCG	D39	5’ upstream of *ftsZ*
TT204	CGTATGTATTCAAATATATCCTCCTCACAATTTATTTTTCCTCTTTATTCGTCAAACATG		

TT205	TTGACGAATAAAGAGGAAAAATAAATTGTGAGGAGGATATATTTGAATACATACGAACA	IU4888	Middle-*aad9* +extra 9 bp of 3' *mreD*
TT206	CTCGACTGGAGAAACGACTGAATGTCGTTCTTATAATTTTTTTAATCTGTTATTTAAA		
TT207	ACAGATTAAAAAAATTATAAGAACGACATTCAGTCGTTTCTCCAGTCGAGCG	D39	87bp 3' *ftsZ*+stop + downstream region
TT166	TCATTGGGAGAGCCGGTTCCTGTGAAGAAT		
For construction of IU8122 (Δ*bgaA*::*tet*-P_{Zn}-RBS^{ftsA}-*ftsZ*$^{+}$)			
TT657	CGCCCCAAGTTCATCACCAATGACATCAAC	pJWV25[f]	*bgaA'*::*tet*-P_{Zn}-RBS^{ftsA}
AJP32	ACATCGCTTCCTCTCTATCTTCCTTGTTATAATAGATTTATGAACACCTTGTTCATTATC		
AJP33	AACAAGGTGTTCATAAATCTATTATAACAAGGAAGATAGAGAGGAAGCGATGTAATGA	IU7054	RBS^{ftsA}-*ftsZ*$^{+}$-*bgaA'*
CS121	GCTTTCTTGAGGCAATTCACTTGGTGC		
For construction of IU9036 (Δ*khpA*)			
P1505	GGGGCATCAATGCCATAAGTGTACTCAAAG	D39	5' flanking fragment with 12 bp of 5' *khpA*
TT732	TCCCGCCCTTCTTATTTTTCAATCGTATCCATCTGTCAACCTACTTTAAACT		
TT733	AGTAGGTTGACAGATGGATACGATTGAAAAATAAGAAGGGCGGGACGG	D39	3' flanking fragment with 6 bp of 3' *khpA*
P1506	GTCATGAATCGGACTCCTACCTGTGTTCGG		
For construction of IU9602 (*khpA-L-FLAG*^{3}-P_{c}-*erm*)			
P1505	GGGGCATCAATGCCATAAGTGTACTCAAAG	D39	5' flanking fragment
JQ135	GCCAGAACCAGCAGCGGAGCCAGCGGAACCTTTTTCGTCAATAACGATTCTTACTTTTTT		
JQ136	AAAAAAGTAAGAATCGTTATTGACGAAAAAGGTTCCGCTGGCTCCGCTGCTGGTTCTGGC	IU4970	L-F^{3}- P_{c}-*erm*
JQ137	CAAAAAAGCGAGACATCCGTCCCGCCCTTCTTATTTCCTCCCGTTAAATAATAGATAACT		
JQ138	AGTTATCTATTATTTAACGGGAGGAAATAAGAAGGGCGGGACGGATGTCTCGCTTTTTTG	D39	3' flanking fragment
P1506	GTCATGAATCGGACTCCTACCTGTGTTCGG		
For construction of IU9621 (Δ*bgaA*::*kan-T1T2*-P_{ftsA}-*khpA*$^{+}$)			
P146	TGGCCATTCATCGCTGGTCGTGCTGAAAT	D39	5' flanking fragment
JQ139	CGCAATAATGAGATTTTCAATCGTATCCATTACATCGCTTCCTCTCTATCTTCCAAGTTT		
JQ140	AAACTTGGAAGATAGAGAGGAAGCGATGTAATGGATACGATTGAAAATCTCATTATTGCG	IU6397	P_{ftsA}-*khpA*$^{+}$ cassette
JQ141	AGCAACTGGTTTATGAGAAAGTAAGTTCTTTTATTTTTCGTCAATAACGATTCTTACTTT		
JQ142	AAAGTAAGAATCGTTATTGACGAAAAATAAAAGAACTTACTTTCTCATAAACCAGTTGCT	D39	3' flanking fragment
CS121	GCTTTCTTGAGGCAATTCACTTGGTGC		

For construction of IU9697 (*khpA-L-FLAG*^{3})			
P1505	GGGGCATCAATGCCATAAGTGTACTCAAAG	IU9602	5’ flanking fragment *khpA*-L-F^3
JQ149	CAAAAAAGCGAGACATCCGTCCCGCCCTTC TTATTTATCATCATCATCTTTATAATCTTT		
JQ150	AAAGATTATAAAGATGATGATGATAAATAAG AAGGGCGGGACGGATGTCTCGCTTTTTTG	D39	3’ flanking fragment
P1506	GTCATGAATCGGACTCCTACCTGTGTTCGG		
For construction of IU9935 (*khpA* (G49A))			
P1505	GGGGCATCAATGCCATAAGTGTACTCAAAG	D39	5’ flanking fragment
JQ151	CCTTACGAGCGATTACACGACCCACATC		
JQ152	GATGTGGGTCGTGTAATCGCTCGTAAGG	D39	3’ flanking fragment
P1506	GTCATGAATCGGACTCCTACCTGTGTTCGG		
For construction of IU9937 (*khpA* (G52A))			
P1505	GGGGCATCAATGCCATAAGTGTACTCAAAG	D39	5’ flanking fragment
JQ153	CTTATCGCAGAAATAGTGCGAGCCTTACGA		
JQ154	TCGTAAGGCTCGCACTATTTCTGCGATAAG	D39	3’ flanking fragment
P1506	GTCATGAATCGGACTCCTACCTGTGTTCGG		
For construction of IU9939 (*khpA*(G49A)-L-FLAG^3)			
P1505	GGGGCATCAATGCCATAAGTGTACTCAAAG	D39	5’ flanking fragment
JQ151	CCTTACGAGCGATTACACGACCCACATC		
JQ152	GATGTGGGTCGTGTAATCGCTCGTAAGG	IU9697	3’ flanking fragment ***khpA*(G49A)-L-FLAG^3**
P1506	GTCATGAATCGGACTCCTACCTGTGTTCGG		
For construction of IU9941 (*khpA*(G52A)-L-FLAG^3)			
P1505	GGGGCATCAATGCCATAAGTGTACTCAAAG	D39	5’ flanking fragment
JQ153	CTTATCGCAGAAATAGTGCGAGCCTTACGA		
JQ154	TCGTAAGGCTCGCACTATTTCTGCGATAAG	IU9697	3’ flanking fragment ***khpA*(G52A)-L-FLAG^3**
P1506	GTCATGAATCGGACTCCTACCTGTGTTCGG		
For construction of IU9977 (*khpA* (G49A G52A))			
P1505	GGGGCATCAATGCCATAAGTGTACTCAAAG	IU9935	5’ flanking fragment ***khpA* (G49A)**
JQ153	CTTATCGCAGAAATAGTGCGAGCCTTACGA		
JQ154	TCGTAAGGCTCGCACTATTTCTGCGATAAG	IU9935	3’ flanking fragment
P1506	GTCATGAATCGGACTCCTACCTGTGTTCGG		

For construction of IU9979 (*khpA*(G49A G52A)-L-FLAG^3)			
P1505	GGGGCATCAATGCCATAAGTGTACTCAAAG	IU9935	5’ flanking fragment ***khpA* (G49A)**
JQ153	CTTATCGCAGAAATAGTGCGAGCCTTACGA		
JQ154	TCGTAAGGCTCGCACTATTTCTGCGATAAG	IU9697	3’ flanking fragment ***khpA*(G52A)-L-FLAG^3**
P1506	GTCATGAATCGGACTCCTACCTGTGTTCGG		
For construction of IU9990 (Δ*bgaA*::*tet*-*P$_{Zn}$*-*pbp2b*$^+$)			
P146	TGGCCATTCATCGCTGGTCGTGCTGAAAT	IU8122	5’ fragment Δ*bgaA*::P$_{zn}$
BR70	GTTAAATTTTCTCATACAAATCAGTCTCATTACATCGCTTCCTCTCTATCTTCCTTGTTA		
BR69	AGGAAGATAGAGAGGAAGCGATGTAATGAGACTGATTTGTATGAGAAAATTTAACAGC	D39	middle fragment *pbp2b*$^+$
BR72	AACTGGTTTATGAGAAAGTAAGTTCTTCTAATTCATTGGATGGTATTTTTGATACAGATT		
BR71	ATATCAAAAATACCATCCAATGAATTAGAAGAACTTACTTTCTCATAAACCAGTTGCTGC	IU8122	3’ fragment
CS121	GCTTTCTTGAGGCAATTCACTTGGTGC		
For construction of IU10091 (*khpA* (R50D K51D))			
P1505	GGGGCATCAATGCCATAAGTGTACTCAAAG	D39	5’ flanking *khpA* (R50D K51D)
JQ155	AGAAATAGTGCGACCATCATCACCGATTAC		
JQ156	GTAATCGGTGATGATGGTCGCACTATTTCT	D39	3’ flanking *khpA* (R50D K51D)
P1506	GTCATGAATCGGACTCCTACCTGTGTTCGG		
For construction of IU10092 (*khpA* (R50D K51D)-L-FLAG^3)			
P1505	GGGGCATCAATGCCATAAGTGTACTCAAAG	D39	5’ flanking *khpA* (R50D K51D)
JQ155	AGAAATAGTGCGACCATCATCACCGATTAC		
JQ156	GTAATCGGTGATGATGGTCGCACTATTTCT	IU9697	3’ flanking *khpA* (R50D K51D)-L-FLAG^3
P1506	GTCATGAATCGGACTCCTACCTGTGTTCGG		

For construction of IU10592 (Δ*khpB*)			
P1539	AGTCGAAACCTTGGGATACGCAGAGATGGA	D39	5’ flanking fragment with 60 bp of 5’ *khpB*
JQ167	TGGCTCATCACCTTCAGAGTAACTAGTCACTAATTCTTTCAATCCTTTCTGGATTGCTTC		
JQ168	GAAGCAATCCAGAAAGGATTGAAAGAATTAGTGACTAGTTACTCTGAAGGTGATGAGCCA	D39	3’ flanking fragment with 60 bp of 3’ *khpB*
P1540	ACCGCTGCACCAATTTGGAATTTGTAGTTA		
For construction of IU10594 (*khpB*-HA)			
P1539	AGTCGAAACCTTGGGATACGCAGAGATGGA	D39	5’ flanking fragment
JQ169	AAACCTGATTTTACTTAAGCATAATCTGGAACATCATATGGATATTCTGTATCTACAACA		
JQ170	TGTTGTAGATACAGAATATCCATATGATGTTCCAGATTATGCTTAAGTAAAATCAGGTTT	D39	3’ flanking fragment
P1540	ACCGCTGCACCAATTTGGAATTTGTAGTTA		
For construction of IU10664 (*khpB-L-FLAG*^{3}-P$_{c}$-*erm*)			
P1539	AGTCGAAACCTTGGGATACGCAGAGATGGA	D39	5’ flanking fragment
JQ185	GCCAGAACCAGCAGCGGAGCCAGCGGAACCTTCTGTATCTACAACAACATAGCGATTTGG		
JQ179	GGTTCCGCTGGCTCCGCTGCTGGTTCTGGC	IU4970	L-F^{3}-P$_{c}$-*erm*
JQ184	TTATTTCCTCCCGTTAAATAATAGATAACTAT		
JQ186	ATAGTTATCTATTATTTAACGGGAGGAAATAAGTAAAATCAGGTTTATCCTGATTTTTTG	D39	3’ flanking fragment
P1540	ACCGCTGCACCAATTTGGAATTTGTAGTTA		
For construction of IU12332 (∆*cozE*:: P$_{c}$-*erm*)			
TT962	CCACCACGGTAAGCAGGCATACCTTCTAAC	D39	5’ flanking fragment with 90 bp of 5’ *cozE*
TT974	ACATTATCCATTAAAAATCAAACGGATCCTACAAAGATCCCATCTGTCTCCATAGGTAAA		
Kan rpsL forward	TAGGATCCGTTTGATTTTTAATGGATAATG	P$_{c}$-*erm* cassette[e]	P$_{c}$-*erm*
Kan rpsL reverse	GGGCCCCTTTCCTTATGCTTTTG		
TT975	GTCCAAAAGCATAAGGAAAGGGGCCCTCCCGTTTGTATGAAAATCATAAAATAATGAAAG	D39	3’ flanking fragment with 60 bp of 5’ *cozE*
TT963	GCCGCTAGACAAGGCTTAATCGTATCTCGC		
For construction of IU12718 (Δ*bgaA*::*kan-T1T2-P*$_{ftsA}$-*ftsA*$^{+}$)			
P146	TGGCCATTCATCGCTGGTCGTGCTGAAAT	IU9621	5’ ∆*bgaA*-*Kan*-T1T2
SC484	GAGCAAAAAAGAAAGCTCTGTGGTAGAAACGCAAAAAGGCCATCCGTCAGG		

SC483	GACGGATGGCCTTTTTGCGTTTCTACCACAGAGCTTTCTTTTTTGCTCTTAGAGAG	D39	P_{ftsA}-*ftsA*$^+$
AJP49	CAACTGGTTTATGAGAAAGTAAGTTCTTTTATTCGTCAAACATGCTTCCGATC		
AJP50	CGGAAGCATGTTTGACGAATAAAAGAACTTACTTTCTCATAAACCAGTTGC	D39	3’ flanking fragment
CS121	GCTTTCTTGAGGCAATTCACTTGGTGC		
For construction of IU12744 (*khpB* (T89A))			
P1539	AGTCGAAACCTTGGGATACGCAGAGATGGA	D39	5’ flanking fragment
JQ300	TGACCAAGGTCAACGGCTTCTTCACTAACC		
JQ299	GGTTAGTGAAGAAGCCGTTGACCTTGGTCA	D39	3’ flanking fragment
P1540	ACCGCTGCACCAATTTGGAATTTGTAGTTA		
For construction of IU12788 (Δ*bgaA*::*kan-T1T2*-P_{Zn}-RBS^{ftsA}-*khpA*$^+$)			
P146	TGGCCATTCATCGCTGGTCGTGCTGAAAT	IU9621	Δ*bgaA*::*kan-T1T2*
JQ145	CCGTATCAGCAAAACCAAAAAAGCCATCTAGTAGAAACGCAAAAAGGCCATCCGTCAGGA		
JQ146	TCCTGACGGATGGCCTTTTTGCGTTTCTACTAGATGGCTTTTTTGGTTTTGCTGATACGG	IU8872	P_{Zn}
JQ147	CGCAATAATGAGATTTTCAATCGTATCCATAAGTTTTTCCTCCTTGTTGATAATTTGTTA		
JQ148	TAACAAATTATCAACAAGGAGGAAAAACTTATGGATACGATTGAAAATCTCATTATTGCG	IU9621	RBS^{ftsA}-*khpA*$^+$
CS121	GCTTTCTTGAGGCAATTCACTTGGTGC		
For construction of IU12929 (Δ*pbp2b*<>P_c-*erm*)			
TT452	GGAGGGTTGGCTGTGGGTGGCTACAAGAAC	D39	5’ flanking fragment
JQ255	CATTATCCATTAAAAATCAAACGGATCCTATTCTAACTTAAAATCTTACTCTTAATTGTA		
Kan rpsL forward	TAGGATCCGTTTGATTTTTAATGGATAATG	P_c-*erm* cassette[e]	P_c-*erm*
Kan rpsL reverse	GGGCCCCTTTCCTTATGCTTTTG		
JQ256	CAAAAGCATAAGGAAAGGGGCCCAAAGGAAATTATGCTTTATCCAACACCTATTGCCAAG	D39	3’ flanking fragment
TT352	TGAAGGACTGGAAAGACCACTGCACCTTCT		
For construction of IU13641 (*ftsA*(ΔUTR))			
TT780	CGCATTACCAAGGAGCAAATAGAGCTTCTTTGGCAGG	D39	5’ flanking fragment
JQ352	AGCCATTACATCGCTTCCTCTCTATCTTCCCACAAAATATTATAACACAAAAAATTTAAT		
JQ353	ATTAAATTTTTTGTGTTATAATATTTTGTGGGAAGATAGAGAGGAAGCGATGTAATGGCT	D39	3’ flanking fragment
TT753	GCCTTCCGCTAATTTGCGAGAGGTTTTCAA		

For construction of IU13881 (*khpB* (T89D))			
P1539	AGTCGAAACCTTGGGATACGCAGAGATGGA	D39	5’ flanking fragment
JQ375	TGACCAAGGTCAACATCTTCTTCACTAACC		
JQ376	GGTTAGTGAAGAAGATGTTGACCTTGGTCA	D39	3’ flanking fragment
P1540	ACCGCTGCACCAATTTGGAATTTGTAGTTA		
For construction of IU13883 (*khpB* (T89E))			
P1539	AGTCGAAACCTTGGGATACGCAGAGATGGA	D39	5’ flanking fragment
JQ377	TGACCAAGGTCAACTTCTTCTTCACTAACC		
JQ378	GGTTAGTGAAGAAGAAGTTGACCTTGGTCA	D39	3’ flanking fragment
P1540	ACCGCTGCACCAATTTGGAATTTGTAGTTA		
For construction of IU14024 (Δ*bgaA*::*kan-T1T2*-P$_{\mathrm{Zn}}$-RBS^{ftsA}-*khpB*$^{+}$)			
P146	TGGCCATTCATCGCTGGTCGTGCTGAAAT	IU12788	Δ*bgaA*::*kan-T1T2*-P$_{\mathrm{Zn}}$-RBS^{ftsA}
JQ239	TTCAACAGTTGAACCTGTAAATACTACCACTACATCGCTTCCTCTCTATCTTCCTTGTTA		
JQ240	TAACAAGGAAGATAGAGAGGAAGCGATGTAGTGGTAGTATTTACAGGTTCAACTGTTGAA	D39	*khpB*$^{+}$
JQ189	AGCAACTGGTTTATGAGAAAGTAAGTTCTTTTATTCTGTATCTACAACAACATAGCGATT		
JQ190	AATCGCTATGTTGTTGTAGATACAGAATAAAAGAACTTACTTTCTCATAAACCAGTTGCT	IU12788	3’ flanking fragment
CS121	GCTTTCTTGAGGCAATTCACTTGGTGC		
For construction of IU14024 (Δ*bgaA*::*kan-T1T2*-P$_{\mathrm{Zn}}$-RBS^{ftsA}-*khpA*$^{+}$-*khpB*$^{+}$)			
P146	TGGCCATTCATCGCTGGTCGTGCTGAAAT	IU12788	Δ*bgaA*::*kan-T1T2*-P$_{\mathrm{Zn}}$-RBS^{ftsA}-*khpA*$^{+}$
JQ385	ACCACTACCAGATTCCTCCTTATTTATTTCTTATTTTTCGTCAATAACGATTCTTACTTT		
JQ386	AAAGTAAGAATCGTTATTGACGAAAAATAAGAAATAAATAAGGAGGAATCTGGTAGTGGT	D39	*khpB*$^{+}$
JQ189	AGCAACTGGTTTATGAGAAAGTAAGTTCTTTTATTCTGTATCTACAACAACATAGCGATT		
JQ190	AATCGCTATGTTGTTGTAGATACAGAATAAAAGAACTTACTTTCTCATAAACCAGTTGCT	IU12788	3’ flanking fragment
CS121	GCTTTCTTGAGGCAATTCACTTGGTGC		

Primers used for qRT-PCR		
Primer name	Sequence (5’ to 3’)	Gene name
AL031	CTGCGACAGCAGATTTGACCACTA	*spd_1874*
AL032	TTCCTGAGGAGCTTCTTCTGCAAC	
AL023	GGAGTAGCTGCCTTGTTTGCAGTA	*spd_0104*

AL024	CAGGGCCATCGATAACCAACTCTT	
JQ235	GCAGATGGCTAATTTCTATG	*spd_0023*
JQ236	CCCCGATTCATTACCAATTT	
JQ237	GGAATCCCTGCTGAATCGTAA	*spd_2067*
JQ238	AAGCTGACCGTGATTTCGTTA	
JQ293	GACTGTCGCTACAATCCGTAATC	*ftsA*
JQ294	GTCACTTCGACTGCTTCTACTTC	
JQ295	CGTGAGCATGTAGACACTCTATTG	*ftsZ*
JQ296	TCTCCACTACCGATACCAATACC	
KK387	CAGCAGTAGGGAATCTTCGGCAAT	16s rRNA
KK388	TACGCCCAATAAATCCGGACAACG	
KK489	AAAGGTCGTGGTGGTAAGGGAATG	*gyrA*
KK490	GCATCTTGATCCAGGCGCATTACT	

Templates and primers used to generate amplicons for transformation assays

amplicon	Strain used for template	primers
Δ*pbp2b*<>*aad9*	IU7397	TT452, TT352
Δ*pbp2b*<>Pc-*erm*	IU12929	TT452, TT352
Δ*mreCD*<>*aad9*	IU10651	AL35, AL17
Δ*rodZ*<>*aad9*	IU10657	TT329, P1385
Δ*rodA*::Pc-*erm*	IU10943	P1543, P1544
Δ*mltG*::Pc-*erm*	IU7260[g]	P1348, P1349
Δ*cozE*::Pc-*erm*	IU12332	TT962, TT963
Δ*gpsB*<>*aad9*	IU4888	TT196, TT197
Δ*pbp1b*::Pc-*erm*	E193	P222, P522

[a] FLAG-tag fusions ((C)-L-FLAG^3) were made to the carboxyl-ends (C) of reading frames. The amino acid sequence of the FLAG epitope is DYKDDDDK (Ramos-Montanez *et al*., 2008; Wayne *et al*., 2010). The FLAG-tag used in this study contained a linker sequence (L; GSAGSAAGSG) followed by three tandem copies of the FLAG epitope (FLAG^3). HA-tag fusions ((C)-HA) were made to the carboxyl-ends (C) of reading frames. The amino acid sequence of the HA epitope is YPYDVPDYA (Wilson *et al.*, 1984).

[b] Antibiotic resistance markers: Erm^R, erythromycin; Kan^R, kanamycin; Spc^R, spectinomycin; Str^R, streptomycin; Tet^R, tetracycline.

[c] IU1824 (Δ*cps rpsL1*) picked up a spontaneous GC→TA drift mutation 4 bp upstream of the -35 box of the P_{ftsA} promoter (-119 bp upstream of the *ftsA* start codon), in a region that does not contain apparent regulatory direct or indirect repeats. FtsA expression is comparable in IU1824 and IU1945, which lacks the drift mutation (data not shown).

[d] Genomic DNA of indicated *S. pneumoniae* strains was used as templates for PCR reactions, except for P_c-[*kan-rpsL*$^+$] and P_c-*erm* cassettes.

[e] P_c-*erm* and P_c-[*kan-rpsL*$^+$] cassettes are described in (Tsui *et al.*, 2011).

[f] pJWV25 (Eberhardt *et al.*, 2009).

[g] IU7260 (Tsui *et al*., 2016)

Table S2. Spontaneous suppressor mutations in D39 Δ*cps* Δ*pbp2b* strains identified by Illumina whole-genome or conventional sequencing[a]

Strain[b]	Gene and mutation	Annotated protein function
sup1 (IU7476)	*spd_0268* (S189C) *spd_0675* (ΔA at K71) *crcB1* (S72L)	CAAX amino terminal protease family protein KH domain protein CrcB family protein
sup6 (IU12015)	Ω(*ddl'-ylmH'*)	Contains chromosomal duplication of the *ftsA-ftsZ* region (see Fig. S5)
sup7 (IU11970)	*spd_1849* (ΔC at Q270)	KhpB RNA binding protein (see Fig. 1B and text)
sup8 (IU11971)	*spd_1849* (ΩA at I102)	KhpB RNA binding protein (see Fig. 1B and text)
sup9 (IU11975)	*spd_1849* (E143-STOP)	KhpB RNA binding protein (see Fig. 1B and text)
sup10 (IU12013)	spd_0675 (M1-STOP)	KhpA RNA binding protein (see Fig. 1A and text)

[a] Illumina MiSeq (IU7476) or NextSeq (IU12015) whole-genome sequencing was performed as described in Experimental procedures. Conventional sequencing of *khpA* and *khpB* was performed on strains IU11970, IU11971, IU11975, and IU12013.

[b] Strains IU7476, IU12015, IU11970, IU11971, IU11975, and IU12013) were isolated from the small number of colonies that arose following independent transformations of unencapsulated strain IU1945 (D39 Δ*cps*) with a Δ*pbp2b<>aad9* amplicon (see text and Supplemental Table S1).

Table S3. mRNA-Seq results for a Δ*khpA* mutant[a]

Δ*khpA* mutant (IU9036) relative to the wild-type parent strain (IU1824)				
SPD number	**Gene name**	**Protein function**	**Fold change**	**FDR[b]**
Increased relative transcript amounts				
WalRK regulon				
0104	-	LysM domain protein	9.0	1.95E-22
0703	-	Conserved hypothetical protein, putative SEDS protein	7.3	1.77E-32
1871	-	Conserved hypothetical membrane protein	3.9	0.03
1874	-	LysM domain protein	19.8	1.03E-70
2043	*pcsB*	Secreted putative N-acetylmuramoyl-l-alanine amidase/endopeptidase	4.1	2.80E-28
Stress protein				
0308	*clpL*	ATP-dependent Clp protease, ATP-binding subunit	1.9	8.51E-03
0458	*hrcA*	Heat-inducible transcription repressor	1.8	3.46E-05
0459	*grpE*	Heat shock protein GrpE	2.3	2.15E-03
0460	*dnaK*	Molecular chaperone DnaK	2.3	1.87E-09
Others				
0775	-	Hypothetical protein	2.0	1.21E-02
0803	-	Hypothetical protein	2.7	1.48E-05
1167	-	ABC transporter, ATP-binding protein	1.8	3.80E-03
1196	*mecA*	Adaptor protein	1.9	7.53E-03
1984	-	Hypersensitive-induced reaction protein 4	2.6	5.99E-06
Decreased relative transcript amounts				
0492	-	Acetyltransferase, GNAT family protein	-2.3	1.21E-02
0675[c]	*khpA*	KH domain protein	-366.0	1.77E-32
0720	-	Amino acid ABC transporter, ATP-binding protein	-2.0	4.31E-04
0887	-	Amino acid permease family protein	-1.9	3.67E-02
0888	*lmb*	Adhesion lipoprotein	-2.2	1.77E-02
0889	*phtD*	Pneumococcal histidine triad protein D precursor	-2.0	2.77E-08

[a] RNA preparation and mRNA-Seq analyses were performed as described in Experimental procedures. RNA was prepared from cultures of strains IU1824 (WT) and IU9036 (Δ*khpA*) grown exponentially in BHI broth to OD_{620} to ≈0.15-0.2. Fold changes

and false discovery rates (FDR) are based on three independent biological replicates. Cut-off limits were 1.8-fold and an FDR value<0.05. Complete mRNA-Seq procedures and data are deposited in the GEO database (accession number GSE101583).

Because of its size, **“Table S4**. KhpA and KhpB RIP-Seq results” is appended to the end of the Supplemental Materials.

SUPPLEMENTAL FIGURE LEGENDS

Fig. S1. Model of PG biosynthesis in ovococcus bacteria, such as *S. pneumoniae*, and topology of proteins involved in peripheral PG synthesis. **(A)** Top. Ovococci divide perpendicularly to their long axis (Zapun *et al.*, 2008). Unencapsulated derivatives of serotype 2 strain D39 *S. pneumoniae* form mostly diplococci and chains of two cells, whereas capsulated D39 strains form short chains of 8–10 cells (Barendt *et al.*, 2009). Bottom. Formation of prolate-ellipsoid-shaped bacteria requires two modes of PG synthesis, peripheral (sidewall-like) and septal PG synthesis, that occur in the midcell region of dividing *S. pneumoniae* cells (Zapun et al., 2008, Sham *et al.*, 2012, Massidda *et al.*, 2013, Pinho *et al.*, 2013, Fleurie *et al.*, 2014, Tsui *et al.,* 2014,). At the start of a division cycle, components of both peripheral PG synthesis complexes (orange ovals) and septal synthesis complexes (green rectangles) locate to the equators of cells (bottom). Peripheral PG synthesis (light blue; top) occurs between the future equator and septum of dividing cells and may commence before septal synthesis (Zapun *et al*., 2008, Wheeler *et al.*, 2011, Massidda *et al*., 2013). At some point, septal PG synthesis (medium blue) commences to divide the cell in two. The complexes that carry out peripheral and septal PG synthesis locate to a large constricting ring throughout the division cycle, with the exception of PBP2x, which moves to the centers of septa in mid-to-late divisional cells (Tsui *et al*., 2014, Rued *et al.,* 2017). The grey Pac-Man symbol corresponds to PG hydrolases that remodel the PG and allow septal separation. Reproduced from (Tsui *et al*., 2016). **(B)** Topology of proteins (not drawn to scale) known or speculated to be involved in peripheral PG synthesis in ovococci (Massidda *et al.*, 2013, Philippe *et al.*, 2014,). Involvement of RodA (bPBP2b regulator/flippase/PG transglycosylase), bPBP2b (PG transpeptidase), MltG (endo-lytic transglycosylase), aPBP1a (PG transglycosylase and transpeptidase), and CozE, MreC, MreD, and RodZ (regulators) in peripheral PG synthesis in *Streptococcus pneumoniae* was shown experimentally in previous studies (Land & Winkler, 2011, Berg *et al.,* 2013, Massidda *et al*., 2013, Philippe *et al.,* 2014, Tsui *et al*., 2014, Fenton *et al*., 2016, Tsui *et al.*, 2016, Rued *et al.*, 2017, Straume *et al.,* 2017). Figure was modified from Tsui *et al.*, 2016. See text for additional details.

Fig. S2. KhpA and KhpB are conserved in important Gram-positive pathogenic bacteria. Partial evolutionary trees are shown for widely distributed KhpA (top) and KhpB (bottom). Sequences of KhpA and KhpB homologs were found in the NCBI database by BLAST searches. Evolutionary trees were generated for a subset of the homologs by using the Phylogeny program (http://www.phylogeny.fr/).

Fig. S3. Δ*khpA* reduces growth rate and cell size of encapsulated D39 and TIGR4 *Streptococcus pneumoniae* strains. **A.** Growth curves with doubling times (DT) in BHI broth of encapsulated D39 *cps*$^+$ wild-type (WT) (IU1690) and Δ*khpA cps*$^+$ (IU9600) strains. **B.** Representative phase-contrast images of encapsulated D39 WT and Δ*khpA* strains. **C.** Growth curves with doubling times (DT) in BHI broth of encapsulated TIGR4 *cps*$^+$ WT (IU11966) and *cps*$^+$ Δ*khpA* (IU13483) strains. **D.** Representative phase-contrast images of encapsulated TIGR4 WT and Δ*khpA* strains. Growth and microscopy of exponentially growing cells were performed as described for Figure 2. The experiment was performed twice with similar results. Scale bar = 1 μm.

Fig. S4. The *mltG*(Y488D) Δ*khpA* double mutant grows slower than either *mltG*(Y488D) or Δ*khpA* single mutant. Growth curves with doubling times (DT) in BHI broth of wild-type (WT) (IU1824), Δ*khpA* (IU9036), *mltG*(Y488D) (IU9760), Δ*khpA* *mltG*(Y488D) (IU12288) strains were determined as described for Figure 2. The experiment was performed three times with similar results.

Fig. S5. Δ*khpA* suppresses Δ*pbp2b*, Δ*mreCD*, Δ*rodZ,* Δ*rodA*, and Δ*gpsB* mutations in the D39 genetic background. WT (IU1824), Δ*khpA* (IU9036), Δ*khpA* Δ*pbp2b* (IU9763), Δ*khpA* Δ*mreCD* (IU10657), Δ*khpA* Δ*rodZ* (IU10659), Δ*khpA* Δ*rodA* (IU13436), and Δ*khpA* Δ*gpsB* (IU12883) mutants were used in these experiments. **A.** Growth curves in BHI broth. Doubling times (DT) were calculated from 3 independent growth curves for cells growing exponentially (OD_{620}=0.03-0.3). Growth curves and doubling times were comparable for Δ*khpB* single and Δ*khpB* (Δ*pbp2b*; Δ*mreCD*; Δ*rodZ*; or Δ*rodA*) double mutants (data not shown). **B.** Representative phase-contrast images of cells in early exponential phase (OD_{620}= 0.10-0.15). The median aspect ratio (AR) and relative cell volume (RV) are indicated for the WT, Δ*khpA*, and Δ*khpA* Δ*pbp2b* mutants determined from 2 independent experiments as described in Figure 2D. Scale bar = 1 μm.

Fig. S6. Absence of growth and morphology defects of strains expressing KhpA-L-FLAG^3 or KhpB-L-FLAG^3 from their native chromosomal loci. **A.** Growth curves in BHI broth of wild-type (WT) (IU1945), *khpA*-L-FLAG^3 (IU9602), and *khpB*-L-FLAG^3 (IU10664) strains. **B.** Representative phase-contrast images of WT, *khpA*-L-FLAG^3, and *khpB*-L-FLAG^3 strains. Growth and microscopy of exponentially growing cells were performed as described for Figure 2. The experiment was performed twice with similar results. Scale bar = 1 μm.

Fig. S7. Similar growth and cell morphology of the Δ*khpA* Δ*khpB* double and Δ*khpA* Δ*khpB* Δ*pbp2b* triple mutants. **A.** Growth curves with doubling times (DT) in BHI broth of WT (IU1824), Δ*khpA* Δ*khpB* (IU10596), and Δ*khpA* Δ*khpB* Δ*pbp2b* (IU10626) strains. **B.** Representative phase-contrast images of WT, Δ*khpA* Δ*khpB*, and Δ*khpA* Δ*khpB* Δ*pbp2b* strains. Growth and microscopy of exponentially growing cells were performed as described for Figure 2. The experiment was performed twice with similar results. Scale bar = 1 μm.

Fig. S8. KhpA and KhpB co-localize at all stages of the bacterial cell cycle. **A**. Representative phase-contrast and fluorescence images of strain IU10602 (*khpA*-L-FLAG^3 *khpB*-HA) grown exponentially in BHI broth and processed for dual-protein 2D immunofluorescence microscopy IFM and DAPI labelling as described in Experimental procedures. **B**. Images of cells were binned into division stages 1–4, and images from the indicated number of cells (n) from two independent biological replicates were averaged using the IMA-GUI program as described previously (Land et al., 2013). Row 1, cell shapes from phase-contrast images; row 2, nucleoid locations from DAPI labelling; row 3, KhpB locations from IFM; row 4, KhpA locations from IFM; row 5, normalized mean fluorescence intensity distributions along the horizontal cell axis for each channel (black, phase image; blue, DNA; green, KhpB; red, KhpA). Comparator 1 from (Tsui *et al*., 2014). 2D IFM averages showing the co-localization of StkP and Pbp2b, which form distinct, highly localized rings during each division stage, in contrast to the diffuse localization of KhpA and KhpB in early divisional cells. **C**. Demographs of cell localization of KhpA (red), and KhpB (green). Cells were aligned based on lengths in phase-contrast images. Graph was generated by MicrobeJ (Ducret *et al*. 2016) for

609 cells. Comparator 2. FtsZ-Myc localization determined by 2D-IFM in a separate experiment, again showing much more distinctive localization of FtsZ than KhpA or KhpB.

Fig. S9. Protein phosphorylation is slightly reduced in Δ*khpA*, Δ*khpA,* and Δ*khpA* Δ*khpB* mutants. Proteins phosphorylated on Thr residues were detected by Western blotting with anti-pThr antibody, and blots were imaged and quantitated as described in Experimental procedures. A representative blot is shown, with background-subtracted luminescence values (mean ± SE; n=2) relative to the wild-type (WT) strain indicated for the StkP/LocZ and DivIVA bands. Lane 1: Ladder; lane 2, WT (IU1824); lane 3, Δ*khpA* (IU9036); lane 4, Δ*khpB* (IU10592); and lane 5, Δ*khpA* Δ*khpB* (IU10596). The band above the DivIVA band in the WT and Δ*khpA* samples, which disappeared in the Δ*khpB* and Δ*khpA* Δ*khpB* mutants, is phosphorylated KhpB (see Ulrych *et al.*, 2016).

Fig. S10. Phosphoablative and phosphomimetic amino acid changes of KhpB at Thr89 (see Fig. 1B) does not affect growth and cell morphology. **A.** Growth curves in BHI broth of wild-type (WT) (IU1824), Δ*khpB* (IU10592), *khpB*(T89A) (IU12744), *khpB*(T89D) (IU13881) and *khpB*(T89E) (IU13883) strains. **B.** Representative phase-contrast images of WT, Δ*khpB*, *khpB*(T89A), *khpB*(T89D) and *khpB*(T89E) strains. Growth and microscopy of exponentially growing cells were performed as described for Figure 2. The D39 experiment was performed twice with similar results. Scale bar = 1 µm.

Fig. S11. Amino acid changes in the KhpA(GXXG) motif destabilizes KhpA and results in a Δ*khpA* phenotype. **A.** Representative Western blots of relative cellular amounts of KhpA-L-FLAG^3 in cells growing exponentially in BHI broth. Numbers are luminescence values relative to the strain expressing wild-type (WT) KhpA-L-FLAG^3 from its native chromosomal locus. Lane 1, ladder; lane 2, untagged *khpA*$^+$ (IU1824) control; lane 3, WT *khpA*-L-FLAG^3 (IU9697); lane 4, *khpA*(G49A)-L-FLAG^3 (IU9939); lane 5, *khpA*(G52A)-L-FLAG^3 (IU9941); lane 6, *khpA*(G49A G52A)-L-FLAG^3 (IU9979); and lane 7, *khpA*(R50D K51D)-L-FLAG^3 (IU10092). **B.** Growth curves with doubling times (DT) in BHI of untagged *khpA* mutants: wild-type (WT) IU1824, Δ*khpA* (IU9036), *khpA*(G49A) (IU9935), *khpA*(G52A) (IU9932), *khpA*(G49A G52A) (IU9977) and *khpA*(R50D K51D) (IU10091) strains. Growth curves were determined as described for Figure 2.

Fig. S12. RIP-qRT-PCR control confirms results and specificity of RIP-Seq experiments. WT (IU1945), *spd_1366*-L-FLAG^3 (IU5809), *khpA*-L-FLAG^3 (IU9602), and *khpB*-L-FLAG^3 (IU10664) strains were used in RIP experiments as described in Experimental procedures. Extracted RNA was reversed transcribed to cDNA and used as templates for qRT-PCR as described in the Experimental procedures*.* Primers for qRT-PCR are listed in Table S1. The relative amounts of the *spd_0023* and *spd_2067* transcripts were significantly enriched by binding to KhpA-L-FLAG^3 or KhpB-L-FLAG^3 compared to the untagged control, similar to the result obtained by RIP-Seq (Table S4A). In contrast, a third putative RNA binding protein, Spd_1366-L-FLAG^3, did not enrich for binding of the *spd_0023* and *spd_2067* transcripts. Means ± SE are shown from three independent experiments. ***P<0.01.

Fig. S13. FtsA is overproduced in the Δ*pbp2b sup6* strain. Western blots of FtsA was performed for the wild-type WT (IU1824), Δ*khpA* (IU9036), Δ*pbp2b sup6* (IU12015; Table S2) strains growing exponentially in BHI broth as described in Experimental procedures. Δ*pbp2b sup6* contains the tandem chromosomal duplication shown in Figure 6. Numbers shown are luminescence intensities relative to the WT strain for this experiment. Western blots of FtsA from the Δ*khpA* mutant were performed numerous times (Fig. 8 and S15; Table 1). The experiment for the Δ*pbp2b sup6* strain was done twice with similar results.

Fig. S14. Relative cellular amount of FtsZ is increased by ≈1.9-fold by ectopic overexpression. Western blots of FtsZ were performed as described in Experimental procedures for strains growing exponentially in BHI broth. Where indicated (+Zn), 0.5 mM $ZnCl_2$ + 0.05 mM $MnSO_4$ were added to the BHI broth. The following strains were assayed: wild-type (WT) (IU1945), $\textit{ftsZ}^+$//P_{ftsA}-$\textit{ftsZ}^+$ (IU7054), Δ*ftsZ*//$P_{\textit{ftsA}}$-ftsZ^+ (IU7814), and $\textit{ftsZ}^+$//P_{Zn}-$\textit{ftsZ}^+$ (IU8122). In strain IU7054, ectopic expression of FtsZ is constitutive from the $P_{\textit{ftsA}}$ promoter, while in strain IU8122, ectopic expression of FtsZ is induced by Zn addition. Ectopic overexpression of *ftsZ* from IU7054, IU8122, or IU12286 failed to suppress Δ*sup2b* (Table 1, line 23; data not shown).

Fig. S15. Ectopic overexpression of *ftsA* does not change relative cellular FtsZ amount. Western blots of the relative amounts of FtsA, FtsZ, and MreC (control) were performed as described in Experimental procedures for cells growing exponentially in BHI broth. The following strains were assayed: wild-type (WT) (IU1824); Δ*khpA* (IU9036); and $\textit{ftsA}^+$//P_{Zn}-$\textit{ftsA}^+$ (IU12310). Where indicated (+Zn), 0.5 mM $ZnCl_2$ + 0.05 mM $MnSO_4$ were added to the BHI broth. Numbers shown are luminescence intensities relative to the WT strain for this experiment.

Fig. S16. FtsA overproduction partially contributed to the phenotypes of Δ*khpA* mutant. WT (IU1824), Δ*khpA* (IU9036), and $\textit{ftsA}^+$//P_{Zn}-$\textit{ftsA}^+$ (IU12310) strains were used in these experiments. -Zn (no addition) or +Zn (addition) of 0.5 mM $ZnCl_2$ and 0.05 mM $MnSO_4$ to final cultures. **A.** Representative phase-contrast images of cells of WT, *ftsA*$^+$//P_{Zn}-*ftsA*$^+$, and Δ*khpA* mutants grown exponentially in BHI broth with or without added Zn. Cells were sampled in early exponential phase (OD_{620} ≈0.10-0.15) from cultures that grew similar to the WT strain with or without added Zn (see Fig. 5B). Addition of Zn to the *ftsA*$^+$//P_{Zn}-*ftsA*$^+$ strain caused a 2.6-fold overexpression of FtsA amount compared to the no Zn addition or the WT strain (see Table 2, lines 1, 2, 5, and 6). Scale bar = 1 µm. **B.** Box and whisker plots (where whiskers indicate 5-95 percentile) of median distributions of cell length, width, aspect ratio (length/width), and relative cell volume of strains growing exponentially in BHI broth with and without Zn addition. Over 100 cells were measured per strain in two independent experiments. **C.** Relative transcript amount of *spd_1874*, which is in the WalRK TCS cell-wall stress regulon, determined by qRT-PCR as described in Experimental procedures. Averages ± SE are shown from 3 independent experiments. For B and C, P values were obtained relative to WT by one-way ANOVA analysis. ** P<0.01 and *** P<0.001.

Fig. S17. Linearity of signal intensity in Western blots versus protein amount in lysates. for FtsA, FtsZ, and MreC. Cell lysates from the wild-type strain (IU1824) were serially diluted, and different amounts of total lysate protein (1.25, 2.50, 5.00, and 10.0 µg) were subjected to Western blotting with detection using anti-FtsA, anti-FtsZ, or anti-MreC antibodies as described in Experimental procedures. The calibration was performed three times independently for each protein. Linear regression was performed using GraphPad Prism program. R^2 values of the fitted lines are >0.96.

Fig. 18. JBrowse profile illustrating enrichment of mRNA near the 5'-UTR and start codon of *ftsA* and mRNA of *sepF* by KhpA-L-FLAG^3 or KhpB-L-FLAG^3 pull down in RIP-Seq experiments compared to the wild-type (WT) control strain, which does not express a FLAG^3-tagged protein. Results from the repeated, independent experimental samples are shown. The JBrowse window from *spd_1481* to *ylmH* indicates that there was no enrichment of *ftsZ* mRNA by KhpA-L-FLAG^3 or KhpB-L-FLAG^3 pull down. Figure S12 shows control experiments that confirm the results and specificity of the RIP-Seq experiments, which are tabulated in Table S4.

Fig. 19. Δ*khpA* and Δ*khpB* mutants are slightly more resistant to gentamicin, but have the same sensitivities to β-lactam antibiotics or tetracycline as the wild-type (WT) strain. Disk diffusion assays were performed as described in Experimental procedures for strains WT (IU1824), Δ*khpA* (IU9036), Δ*khpB* (IU10592), and Δ*khpA* Δ*khpB* (IU10596) strains. Means ± SE are shown from three independent experiments. ***P<0.001.

Fig. S20. The Δ*khpA* Δ*walK* double mutant grows slower than either Δ*walK* or Δ*khpA* single mutant. Growth curves with doubling times (DT) in BHI broth of wild-type (WT) (IU1824), Δ*khpA* (IU9036), Δ*walK* (IU10230), and Δ*khpA* Δ*walK* (IU10080) strains were determined as described for Figure 2. The experiment was performed twice with similar results.

Fig. S21. KhpB overproduction does not alter growth and cell morphology of D39-derived strains. **A.** Growth curves of wild-type (WT) (IU1824) and *khpB*$^+$//P$_{Zn}$-*khpB*$^+$ (IU14024) strains in BHI with or without additional of 0.5 mM $ZnCl_2$ + 0.05 mM $MnSO_4$ (+Zn). **B.** Representative phase-contrast images of WT and *khpB*$^+$//P$_{Zn}$-*khpB* strains growing in BHI with or without Zn addition. Growth and microscopy of exponentially growing cells were performed as described for Figure 2. The experiment was performed twice with similar results. Scale bar = 1 µm.

REFERENCES

Barendt, S.M., Land, A.D., Sham, L.T., Ng, W.L., Tsui, H.C., Arnold, R.J., Winkler, M.E. (2009) Influences of capsule on cell shape and chain formation of wild-type and *pcsB* mutants of serotype 2 *Streptococcus pneumoniae*. *J Bacteriol* **191**: 3024-3040.

Berg, K.H., Stamsas, G.A., Straume D., Havarstein, L.S. (2013) Effects of low PBP2b levels on cell morphology and peptidoglycan composition in *Streptococcus pneumoniae* R6. *J Bacteriol* **195**: 4342-4354.

Ducret, A., Quardokus, E. M., Brun, Y. V. (2016) MicrobeJ, a tool for high throughput bacterial cell detection and quantitative analysis. Nat Microbiol **1**: 16077

Eberhardt, A., L.J. Wu, J. Errington, W. Vollmer & J.W. Veening, (2009) Cellular localization of choline-utilization proteins in *Streptococcus pneumoniae* using novel fluorescent reporter systems. *Mol Microbiol* **74**: 395-408.

Fenton, A. K., Mortaji L, E. I., Lau, D. T., Rudner, D. Z., Bernhardt, T. G. (2017) CozE is a member of the MreCD complex that directs cell elongation in *Streptococcus pneumoniae*. *Nat Microbiol* **2**: 16237

Fleurie, A., Manuse, S., Zhao, C., Campo, N., Cluzel, C., Lavergne, J.P. *et al*. (2014) Interplay of the serine/threonine-kinase StkP and the paralogs DivIVA and GpsB in pneumococcal cell elongation and division. *PLoS Genet* **10**: e1004275

Land, A.D., Winkler, M.E. (2011) The requirement for pneumococcal MreC and MreD is relieved by inactivation of the gene encoding PBP1a. *J Bacteriol* **193**: 4166-4179.

Land, A.D., Tsui, H.C., Kocaoglu, O., Vella, S.A., Shaw, S.L., Keen, S.K. *et al*. (2013) Requirement of essential Pbp2x and GpsB for septal ring closure in *Streptococcus pneumoniae* D39. *Mol Microbiol* **90**: 939-955.

Lanie, J.A., Ng, W.L., Kazmierczak, K.M., Andrzejewsk, T.M., Davidsen, T.M., Wayne, K.J., *et al*. (2007) Genome sequence of Avery's virulent serotype 2 strain D39 of *Streptococcus pneumoniae* and comparison with that of unencapsulated laboratory strain R6. *J Bacteriol* **189:** 38-51.

Massidda, O., Novakova, L., Vollmer, W. (2013) From models to pathogens: how much have we learned about *Streptococcus pneumoniae* cell division? *Environ Microbiol* **15**: 3133-3157.

Mura, A., Fadda, D., Perez, A.J., Danforth, M.L., Musu, D., Rico, A.I., *et al*. (2017) Roles of the essential protein FtsA in cell growth and division in *Streptococcus pneumoniae*. *J Bacteriol* **199**: e00608-16.

Philippe, J., Vernet, T., Zapun, A. (2014) The elongation of ovococci. *Microbl Drug Resist* **20**: 215-221.

Pinho, M.G., Kjos, M., Veening, J.W. (2013) How to get (a)round: mechanisms controlling growth and division of coccoid bacteria. *Nat Rev Microbiol* **11**: 601-614.

Ramos-Montanez, S., Tsui, H.C., Wayne, K.J., Morris, J.L., Peters, L.E., Zhang, F., *et al*. (2008). Polymorphism and regulation of the *spxB* (pyruvate oxidase) virulence factor gene by a CBS-HotDog domain protein (SpxR) in serotype 2 *Streptococcus pneumoniae*. *Mol Microbiol* **67**: 729-746.

Rued, B. E., Zheng, J. J., Mura, A., Tsui, H. T., Boersma, M. J., Mazny, J. L., *et al*. (2017) Suppression and synthetic-lethal genetic relationships of Δ*gpsB* mutations indicate that GpsB mediates protein phosphorylation and penicillin-binding protein interactions in *Streptococcus pneumoniae* D39. *Mol Microbiol* **103**: 931-957

Sham, L.T., Tsui, H.C., Land, A.D., Barendt, S.M., Winkler, M.E. (2012) Recent advances in pneumococcal peptidoglycan biosynthesis suggest new vaccine and antimicrobial targets. *Curr Opin Microbiol* **15**: 194-203.

Straume, D. Stamsas, G. A., Berg, K. H., Salehian, Z., Harvarstein, L. S. (2017) Identification of pneumococcal proteins that are functionally linked to penicillin-binding protein 2b (PBP2b). *Mol Microbiol* **103**: 99-116.

Tsui, H.C., S.K. Keen, L.T. Sham, K.J. Wayne & M.E. Winkler, (2011) Dynamic distribution of the SecA and SecY translocase subunits and septal localization of the HtrA surface chaperone/protease during *Streptococcus pneumoniae* D39 cell division. *mBio* **2**: e00202-11.

Tsui, H.T., Moersma, M.J., Vella, S.A., Kocaoglu, O., Kuru, E., Peceny, J.K., *et al*. (2014). Pbp2x localizes separately from Pbp2b and other peptidoglycan synthesis proteins during later stages of cell division of *Streptococcus pneumoniae* D39. *Mol Microbiol* **94**: 21-40.

Tsui, H.C., Zheng, J.J., Magallon, A.N., Ryan, J.D., Yunck, R., Rued, B.E., *et al*. (2016). Suppression of a deletion mutation in the gene encoding essential PBP2b reveals a new lytic transglycosylase involved in peripheral peptidoglycan synthesis in *Streptococcus pneumoniae* D39. *Mol Microbiol* **100**: 1039-1065.

Wayne, K.J., Sham, L.T., Tsui, H.C., Gutu, A.D., Barendt, S.M., Keen, S.K., Winkler, M.E. (2010). Localization and cellular amounts of the WalRKJ (VicRKX) two-component regulatory system proteins in serotype 2 *Streptococcus pneumoniae. J Bacteriol* **192**: 4388-4394.

Tettelin, H., Nelson, K.E., Paulsen, I.T., Eisen, J.A., Read, T.D., Peterson S., *et al*. (2001). Complete genome sequence of a virulent isolate of *Streptococcus pneumoniae*. *Science* **293**: 498-506

Wheeler, R., Mesnage, S., Boneca, I.G., Hobbs, J.K., Foster, S.J. (2011) Super-resolution microscopy reveals cell wall dynamics and peptidoglycan architecture in ovococcal bacteria. *Molec Microbiol* **82**: 1096-1109.

Ulrych, A., N. Holeckova, J. Goldova, L. Doubravova, O. Benada, O. Kofronova, P. Halada & P. Branny, (2016) Characterization of pneumococcal Ser/Thr protein phosphatase phpP mutant and identification of a novel PhpP substrate, putative RNA binding protein Jag. *BMC Microbiol* **16**: 247.

Wilson, I.A., Niman, H.L., Houghten, R.A., Cherenson, A.R., Connolly, M.L., Lerner, R.A. (1984) The structure of an antigenic determinant in a protein. Cell 37: 767-778.

Zapun, A., Vernet, T., Pinho, M.G. (2008) The different shapes of cocci. *FEMS Microbiol Rev* **32**: 345-360.

Zheng, J.J., Sinha, D., Wayne, K.J., Winkler, M.E. (2016) Physiological roles of the dual phosphate transporter systems in low and high phosphate conditions and in capsule maintenance of *Streptococcus pneumoniae* D39. *Front Cell Infect Microbiol* **6**:63. doi: 10.3389/fcimb.

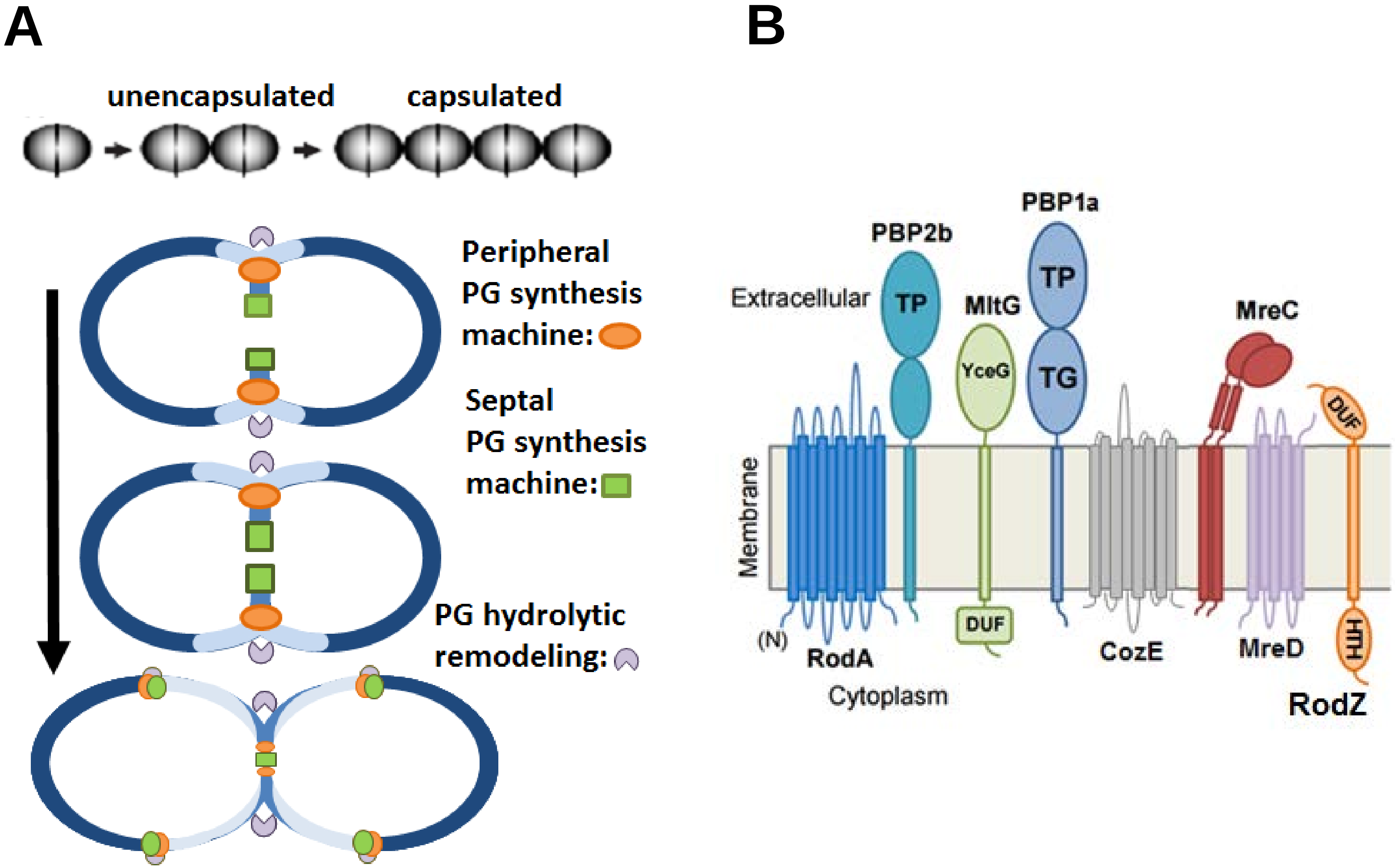
A
unencapsulated
capsulated
Peripheral PG synthesis machine:
Septal PG synthesis machine:
PG hydrolytic remodeling:
B
PBP1a
PBP2b
TP
TP
TG
Extracellular
MltG
YceG
MreC
DUF
Membrane
DUF
(N)
RodA
Cytoplasm
CozE
MreD
HTH
RodZ

Fig. S1

Partial Trees

KhpA

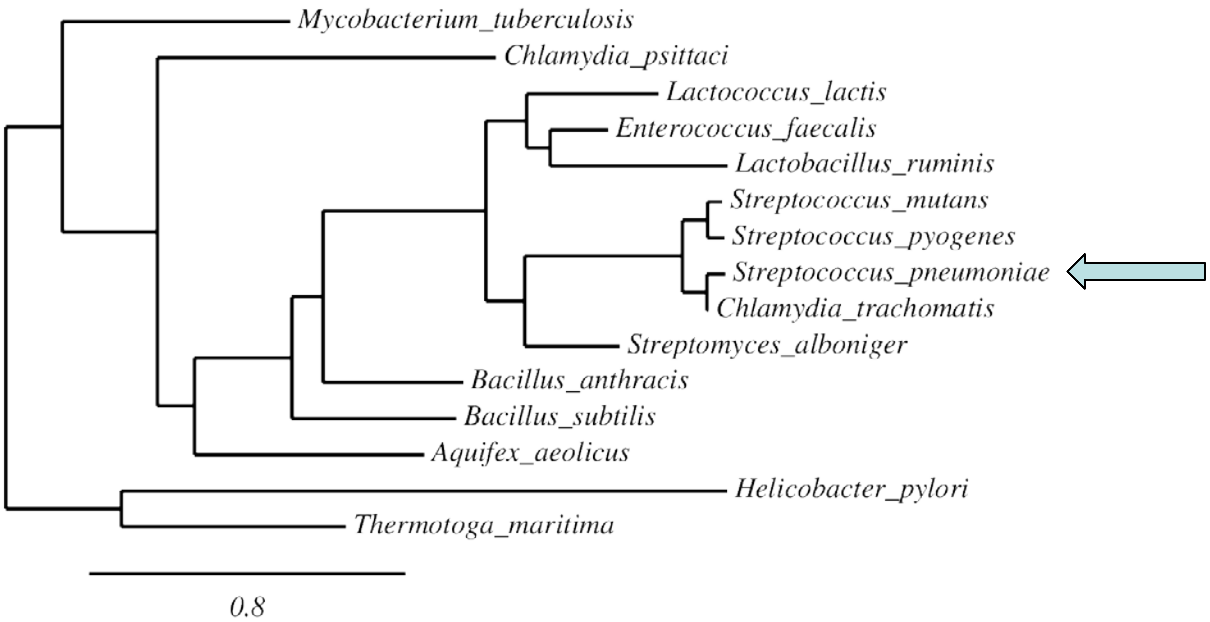

KhpB

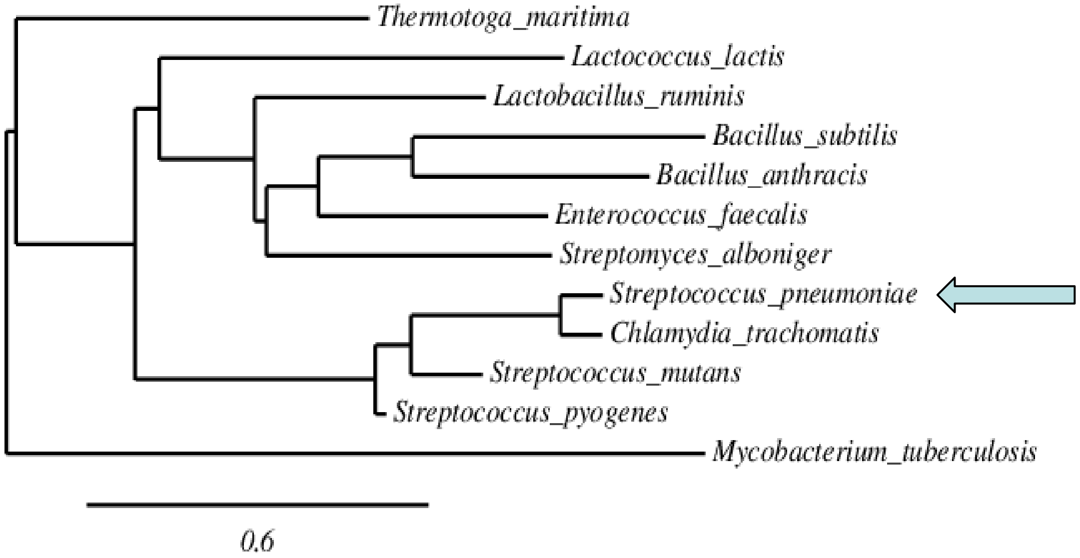

Fig. S2

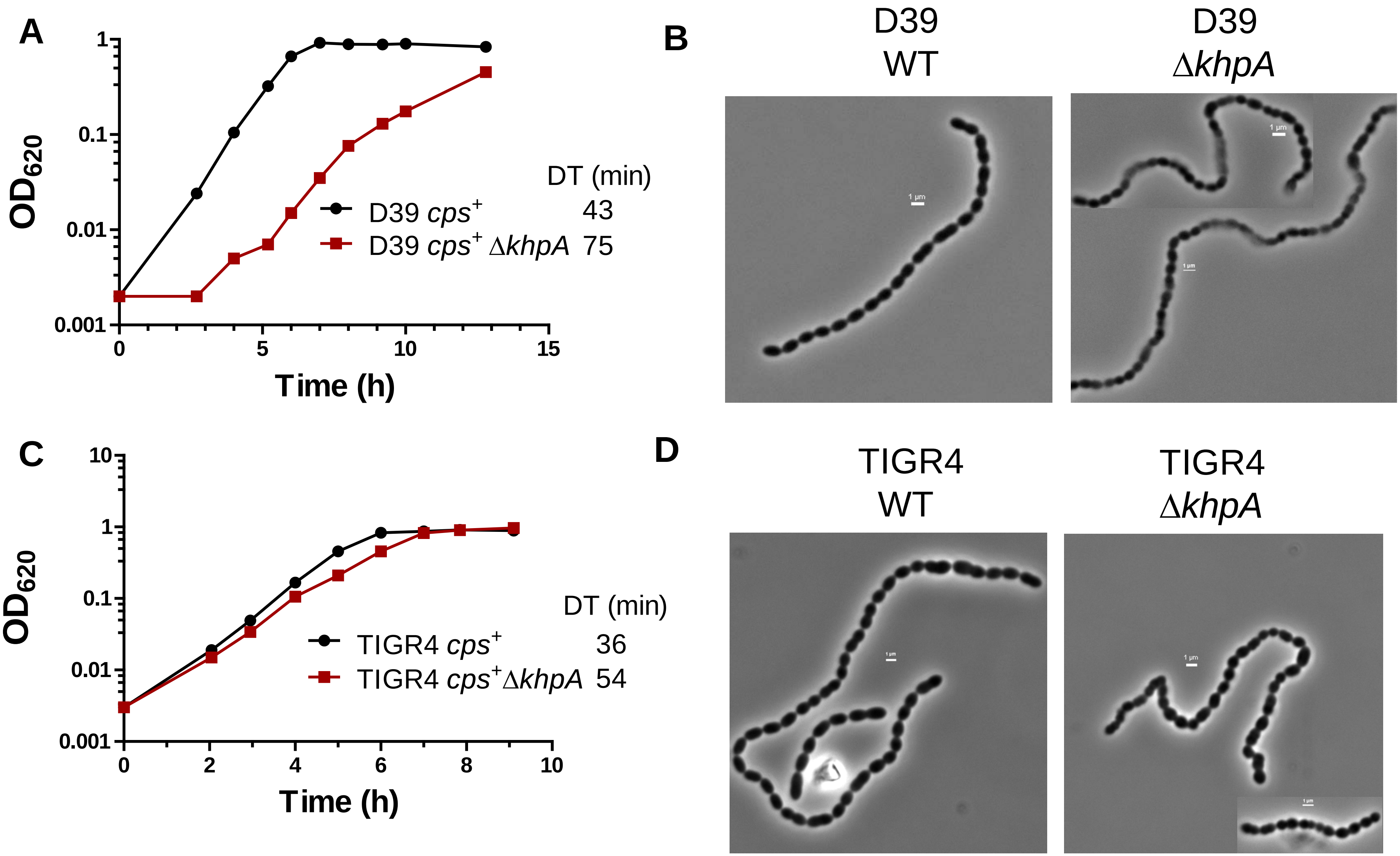A
1
0.1
0.01
0.001
OD_{620}
0
5
10
15
Time (h)
DT (min)
D39 *cps*$^+$ 43
D39 *cps*$^+$ Δ*khpA* 75
B
D39
WT
D39
Δ*khpA*
1 µm
1 µm
1 µm
C
10
1
0.1
0.01
0.001
OD_{620}
0
2
4
6
8
10
Time (h)
DT (min)
TIGR4 *cps*$^+$ 36
TIGR4 *cps*$^+$Δ*khpA* 54
D
TIGR4
WT
TIGR4
Δ*khpA*
1 µm
1 µm
1 µm

Fig. S3

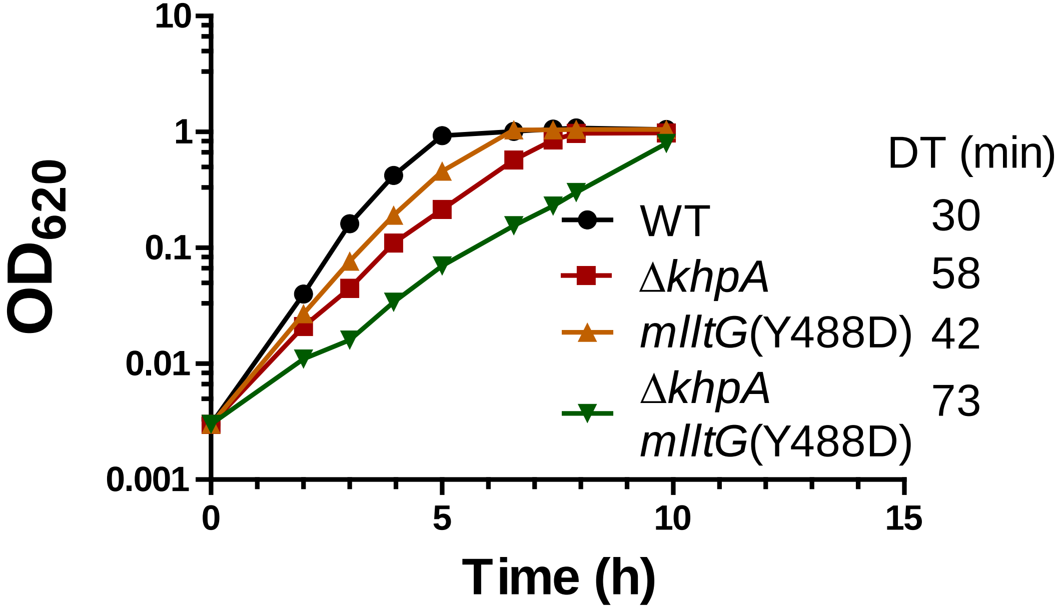
10
1
0.1
0.01
0.001
OD620
0
5
10
15
Time (h)
DT (min)
WT 30
ΔkhpA 58
mlltG(Y488D) 42
ΔkhpA mlltG(Y488D) 73

Fig. S4

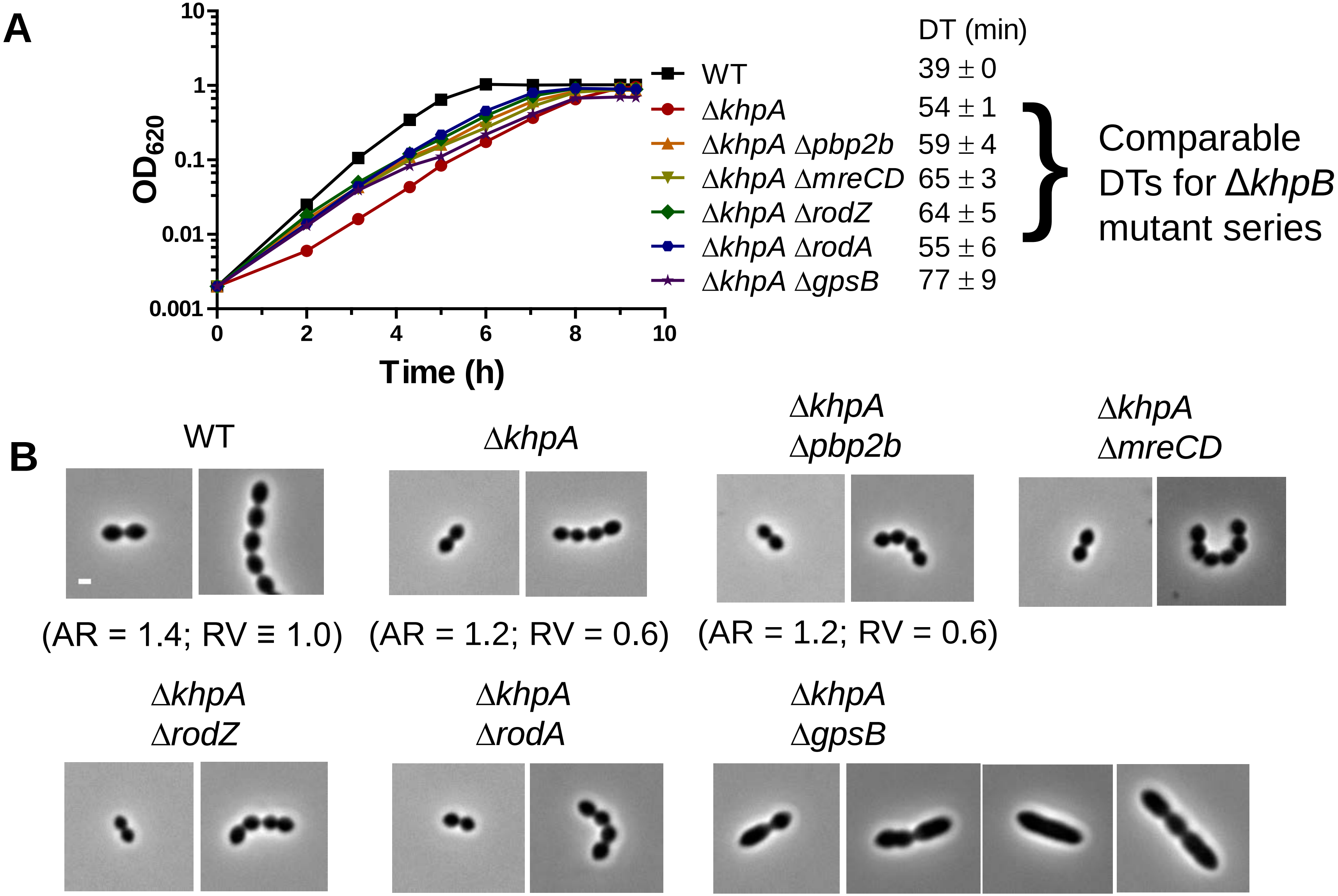
A
OD$_{620}$
10
1
0.1
0.01
0.001
0
2
4
6
8
10
Time (h)
WT
Δ*khpA*
Δ*khpA* Δ*pbp2b*
Δ*khpA* Δ*mreCD*
Δ*khpA* Δ*rodZ*
Δ*khpA* Δ*rodA*
Δ*khpA* Δ*gpsB*
DT (min)
39 ± 0
54 ± 1
59 ± 4
65 ± 3
64 ± 5
55 ± 6
77 ± 9
Comparable DTs for Δ*khpB* mutant series
B
WT
(AR = 1.4; RV ≡ 1.0)
Δ*khpA*
(AR = 1.2; RV = 0.6)
Δ*khpA* Δ*pbp2b*
(AR = 1.2; RV = 0.6)
Δ*khpA* Δ*mreCD*
Δ*khpA* Δ*rodZ*
Δ*khpA* Δ*rodA*
Δ*khpA* Δ*gpsB*

Fig. S5

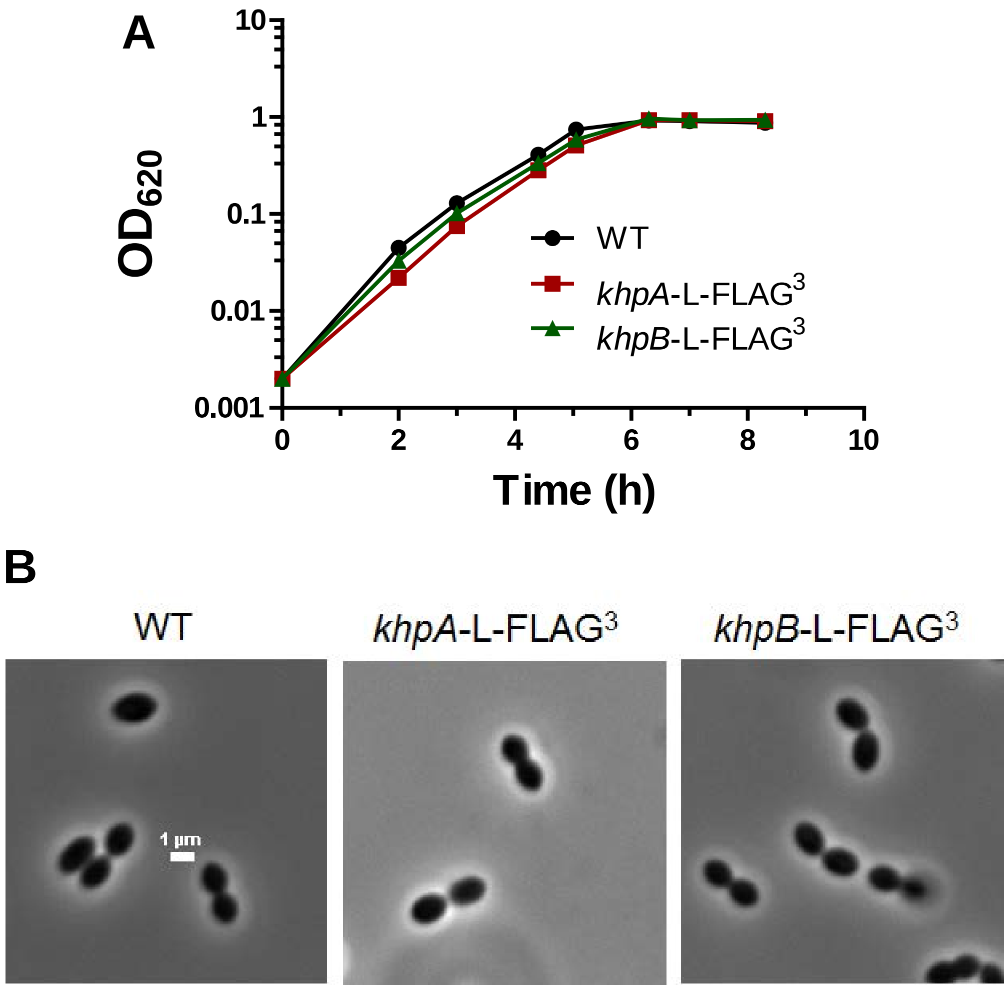
A
10
1
0.1
0.01
0.001
OD620
0
2
4
6
8
10
Time (h)
● WT
■ khpA-L-FLAG3
▲ khpB-L-FLAG3
B
WT
khpA-L-FLAG3
khpB-L-FLAG3
1 µm

Fig. S6

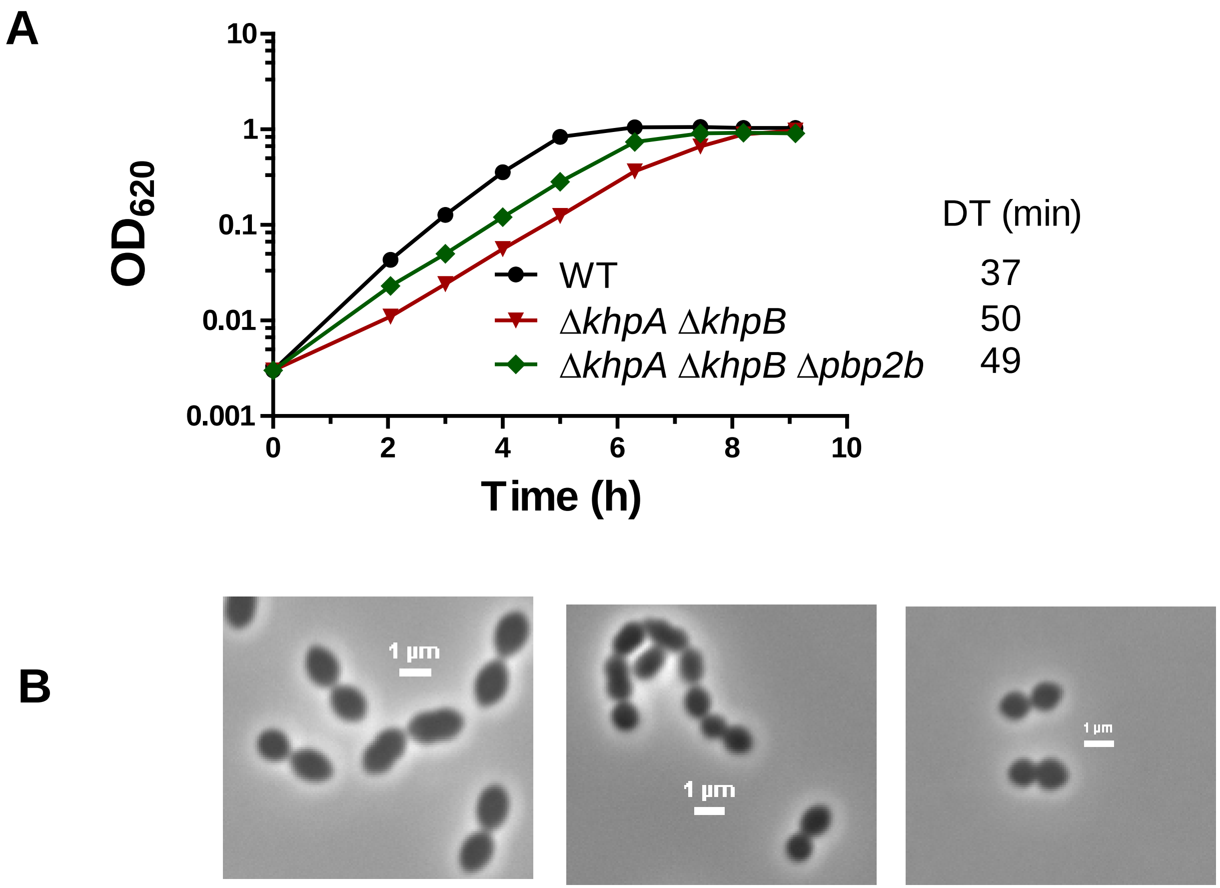

WT

ΔkhpA
ΔkhpB

ΔkhpA
ΔkhpB
Δpbp2b

Fig. S7

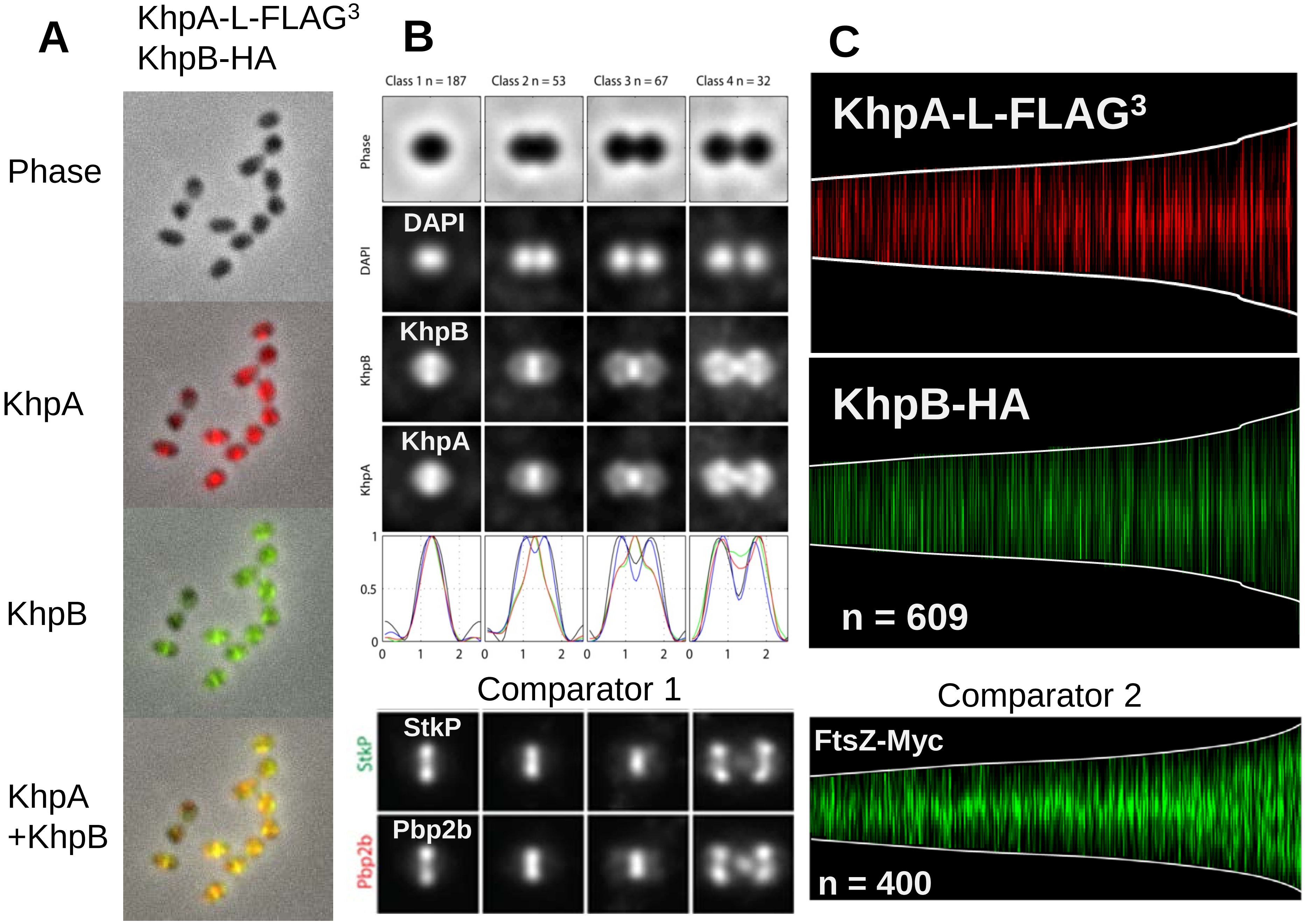
A
KhpA-L-FLAG3
KhpB-HA
Phase
KhpA
KhpB
KhpA
+KhpB
B
Class 1 n = 187
Class 2 n = 53
Class 3 n = 67
Class 4 n = 32
Phase
DAPI
KhpB
KhpA
1
0.5
0
0 1 2
Comparator 1
StkP
Pbp2b
C
KhpA-L-FLAG3
KhpB-HA
n = 609
Comparator 2
FtsZ-Myc
n = 400

Fig. S8

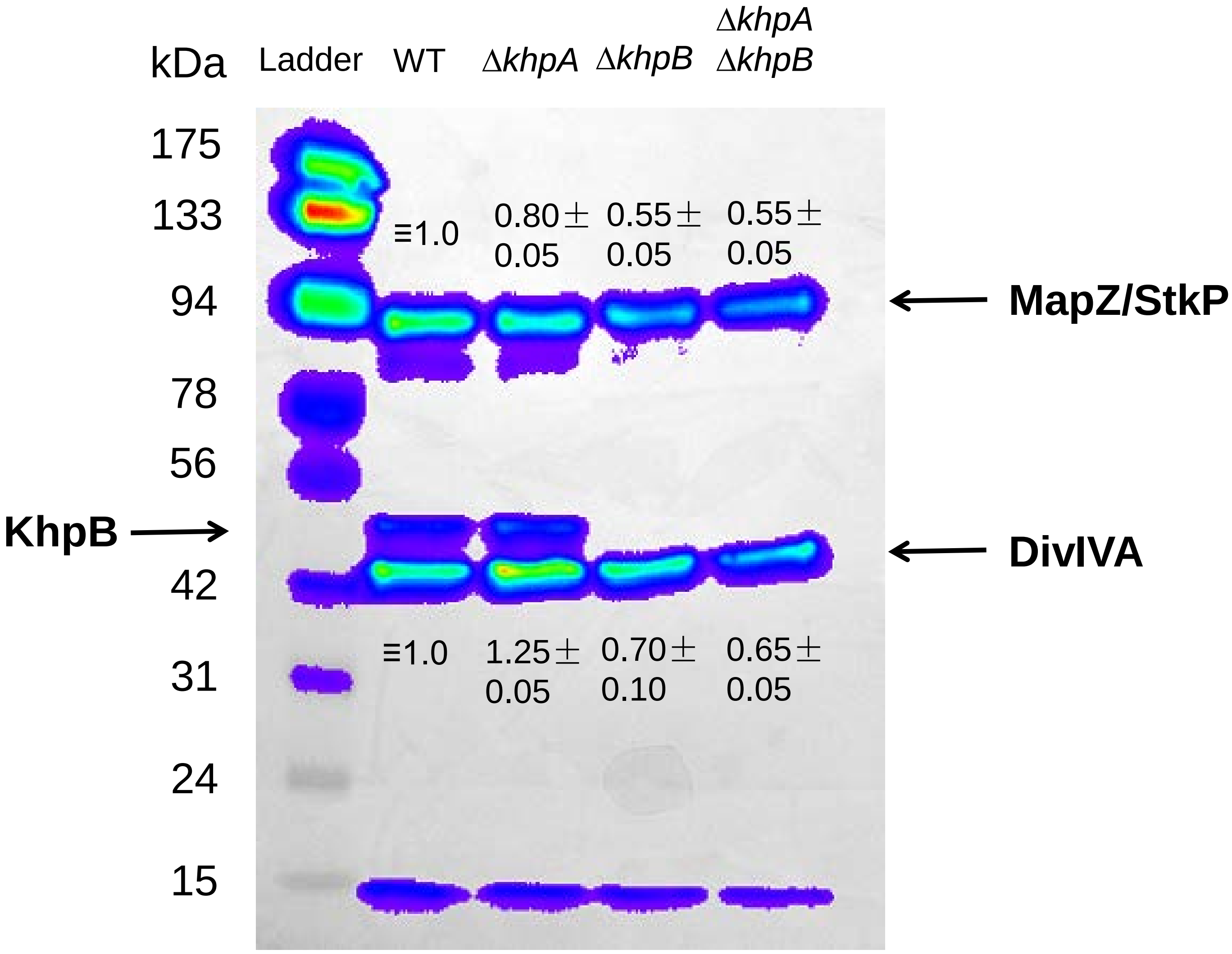
kDa
Ladder
WT
Δ*khpA*
Δ*khpB*
Δ*khpA* Δ*khpB*
175
133
94
78
56
42
31
24
15
≡1.0
0.80± 0.05
0.55± 0.05
0.55± 0.05
MapZ/StkP
KhpB
DivIVA
≡1.0
1.25± 0.05
0.70± 0.10
0.65± 0.05

Fig. S9

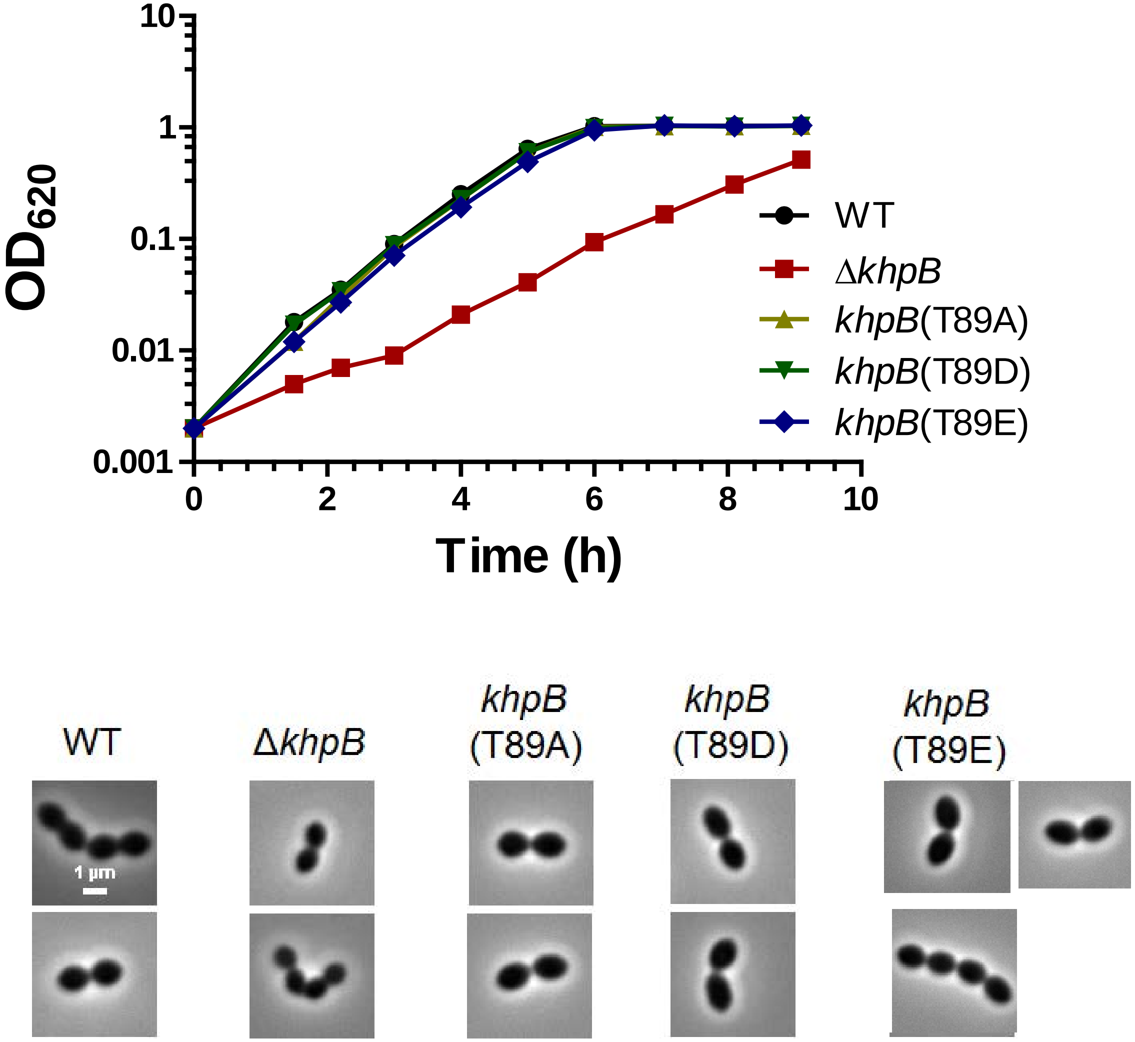
10
1
0.1
0.01
0.001
OD620
0
2
4
6
8
10
Time (h)
WT
ΔkhpB
khpB(T89A)
khpB(T89D)
khpB(T89E)
WT
ΔkhpB
khpB (T89A)
khpB (T89D)
khpB (T89E)
1 µm

Fig. S10

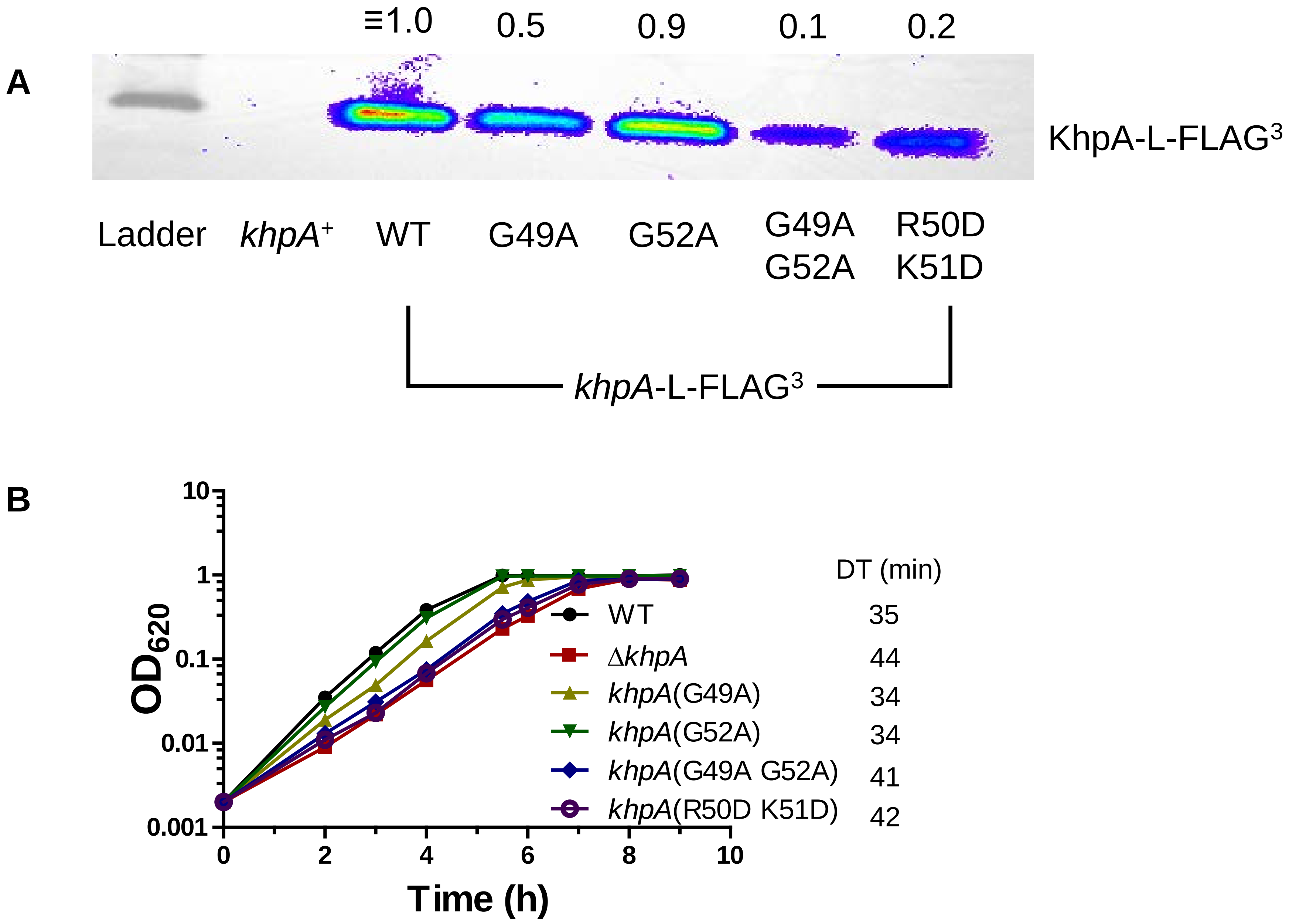
A
≡1.0
0.5
0.9
0.1
0.2
KhpA-L-FLAG^3
Ladder
khpA$^+$
WT
G49A
G52A
G49A G52A
R50D K51D
khpA-L-FLAG^3
B
10
1
0.1
0.01
0.001
OD$_{620}$
0
2
4
6
8
10
Time (h)
DT (min)
WT 35
Δ*khpA* 44
khpA(G49A) 34
khpA(G52A) 34
khpA(G49A G52A) 41
khpA(R50D K51D) 42

Fig. S11

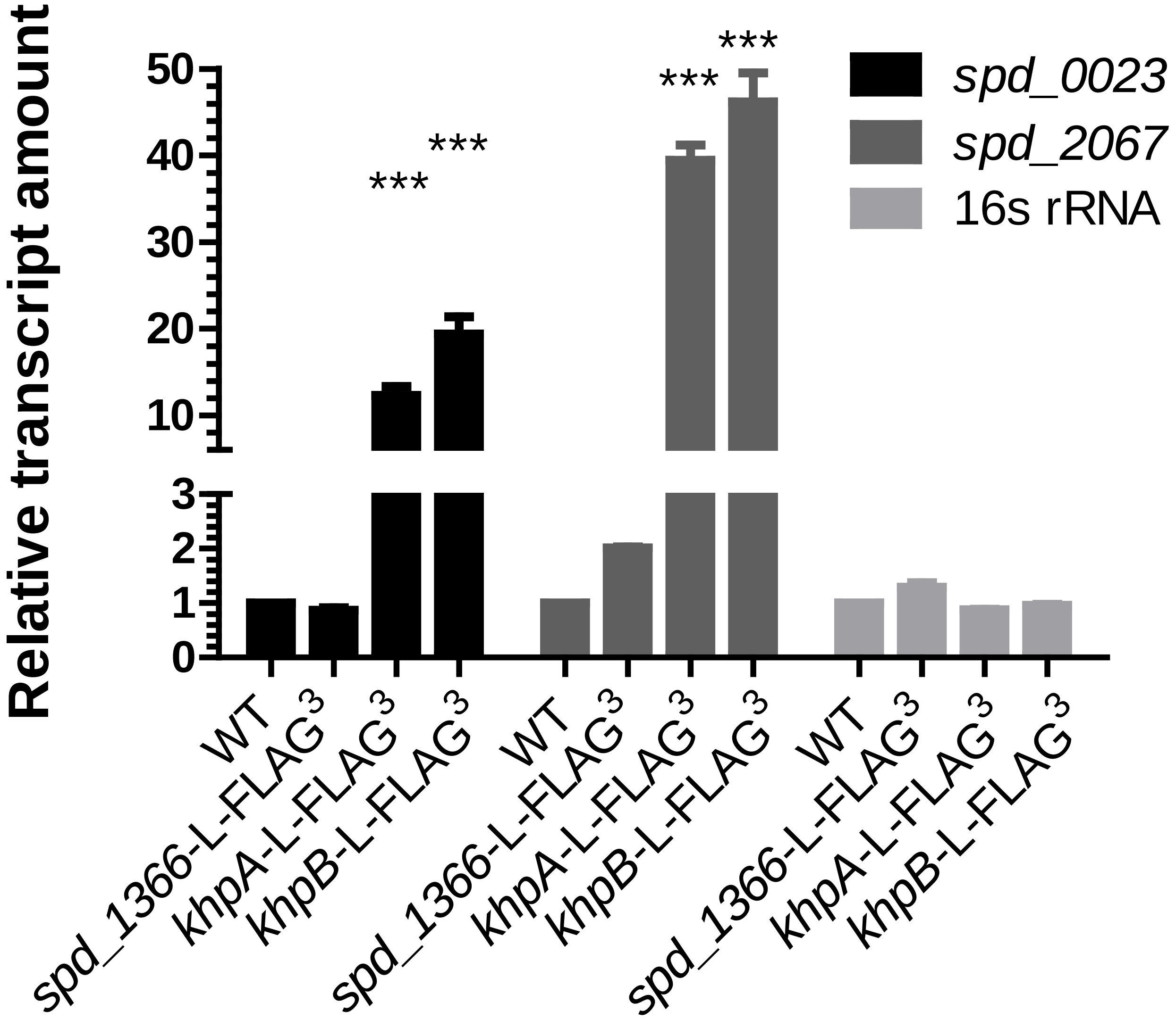
Relative transcript amount
50
40
30
20
10
3
2
1
0
***
***
***
***
spd_0023
spd_2067
16s rRNA
WT
spd_1366-L-FLAG3
khpA-L-FLAG3
khpB-L-FLAG3
WT
spd_1366-L-FLAG3
khpA-L-FLAG3
khpB-L-FLAG3
WT
spd_1366-L-FLAG3
khpA-L-FLAG3
khpB-L-FLAG3

Fig. S12

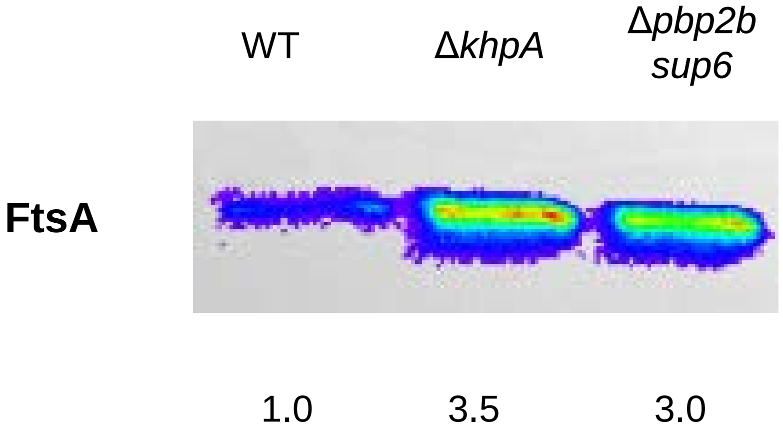

Fig. S13

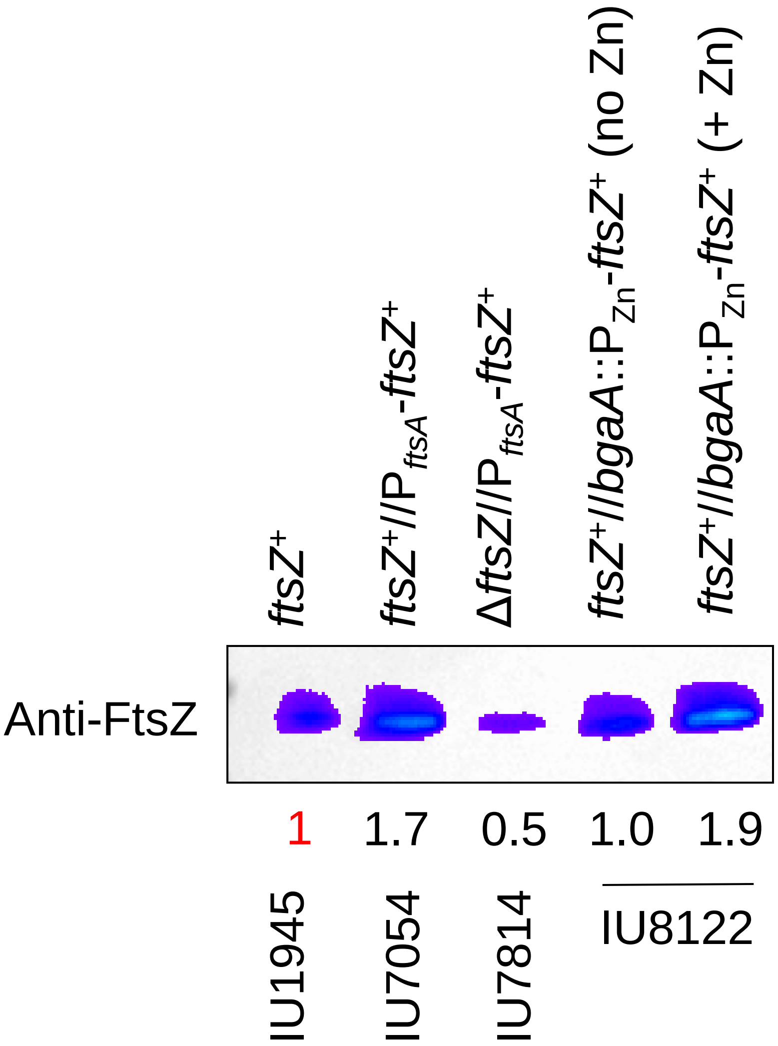
ftsZ$^+$
ftsZ$^+$//P$_{ftsA}$-*ftsZ*$^+$
Δ*ftsZ*//P$_{ftsA}$-*ftsZ*$^+$
ftsZ$^+$//*bgaA*::P$_{Zn}$-*ftsZ*$^+$ (no Zn)
ftsZ$^+$//*bgaA*::P$_{Zn}$-*ftsZ*$^+$ (+ Zn)
Anti-FtsZ
1
1.7
0.5
1.0
1.9
IU1945
IU7054
IU7814
IU8122

Fig. S14

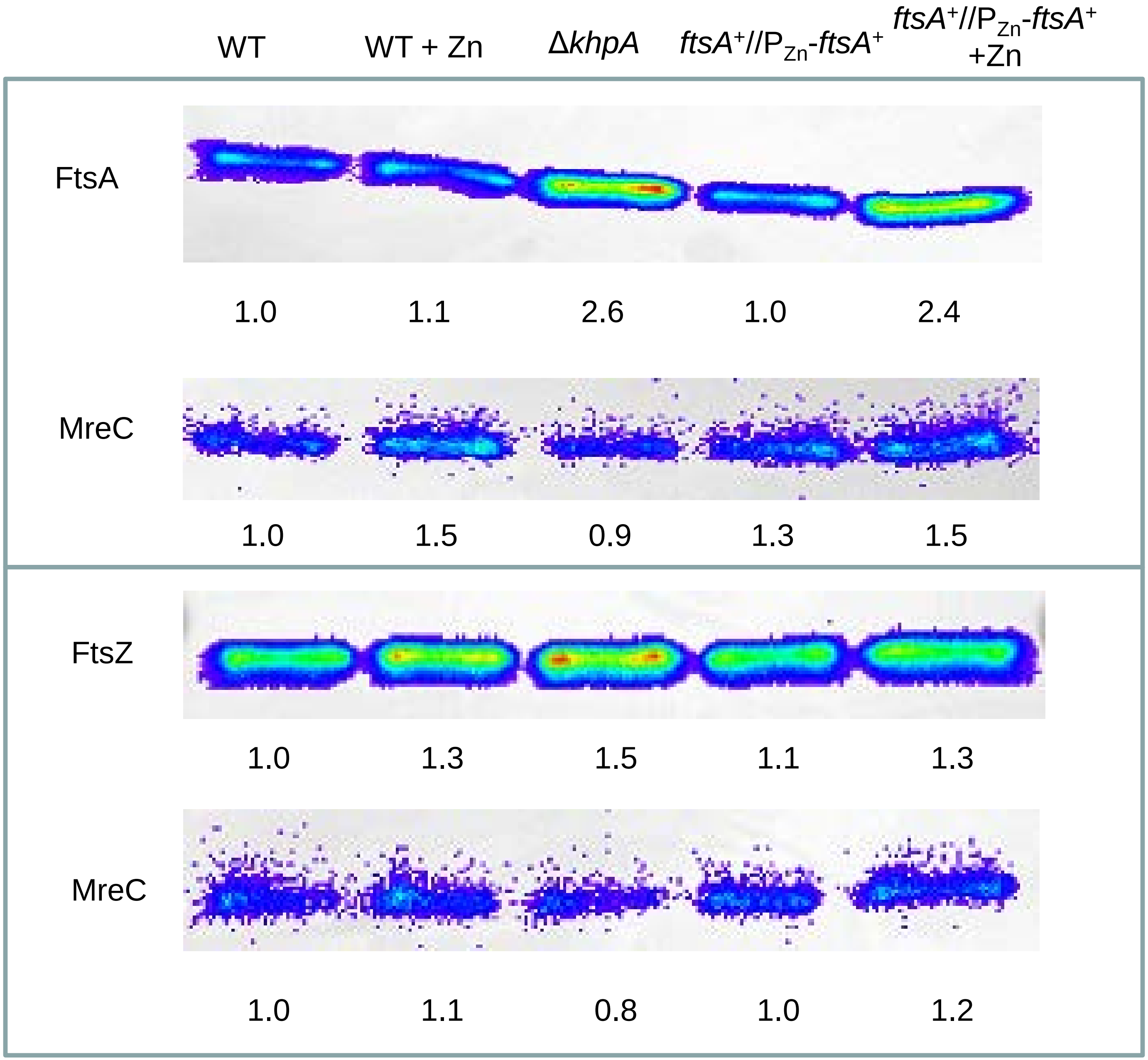
WT
WT + Zn
Δ*khpA*
ftsA$^+$//P_{Zn}-*ftsA*$^+$
ftsA$^+$//P_{Zn}-*ftsA*$^+$ +Zn
FtsA
1.0 1.1 2.6 1.0 2.4
MreC
1.0 1.5 0.9 1.3 1.5
FtsZ
1.0 1.3 1.5 1.1 1.3
MreC
1.0 1.1 0.8 1.0 1.2

Fig. S15

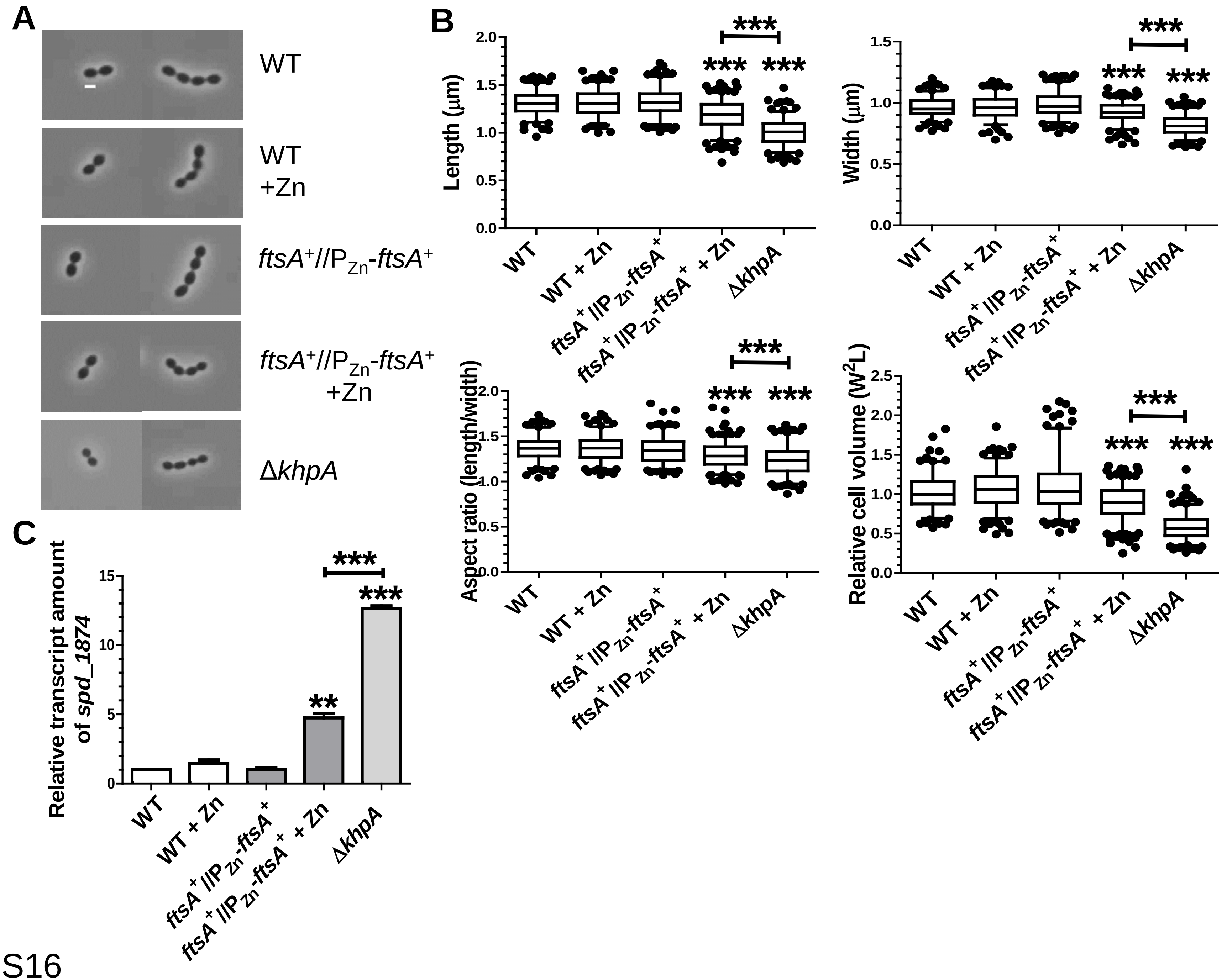
A
WT
WT +Zn
ftsA+//PZn-ftsA+
ftsA+//PZn-ftsA+ +Zn
ΔkhpA
B
Length (µm)
2.0
1.5
1.0
0.5
0.0
Width (µm)
1.5
1.0
0.5
0.0
Aspect ratio (length/width)
Relative cell volume (W2L)
2.5
***
WT
WT + Zn
ftsA+//PZn-ftsA+
ftsA+//PZn-ftsA+ + Zn
ΔkhpA
C
Relative transcript amount of spd_1874
15
10
5
0
**
***

Fig. S16

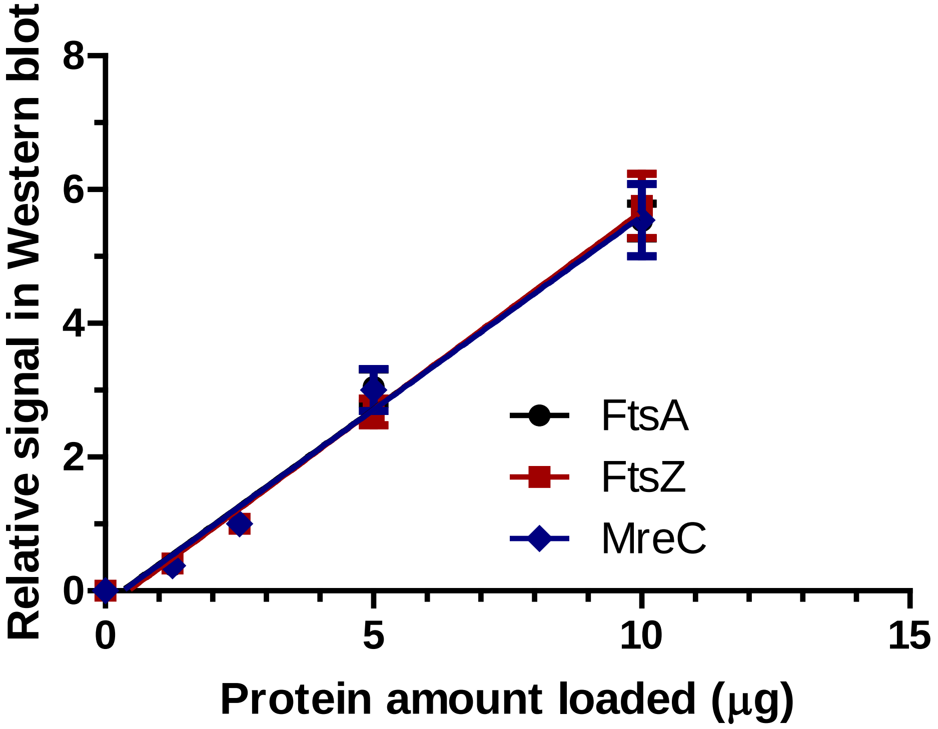
Relative signal in Western blot
8
6
4
2
0
0
5
10
15
Protein amount loaded (μg)
FtsA
FtsZ
MreC

Fig. S17

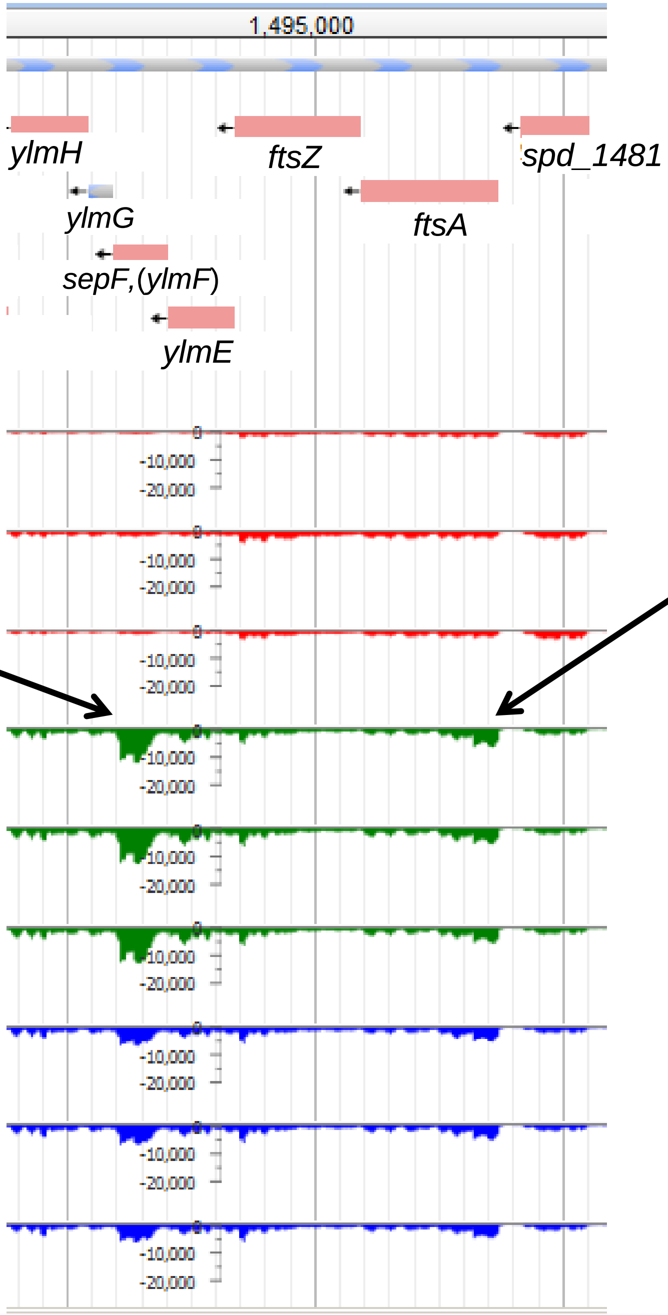

WT

sepF

Region near the 5’-UTR leader and start codon of *ftsA*

khpA-L-F^3

khpB-L-F^3

Fig. S18

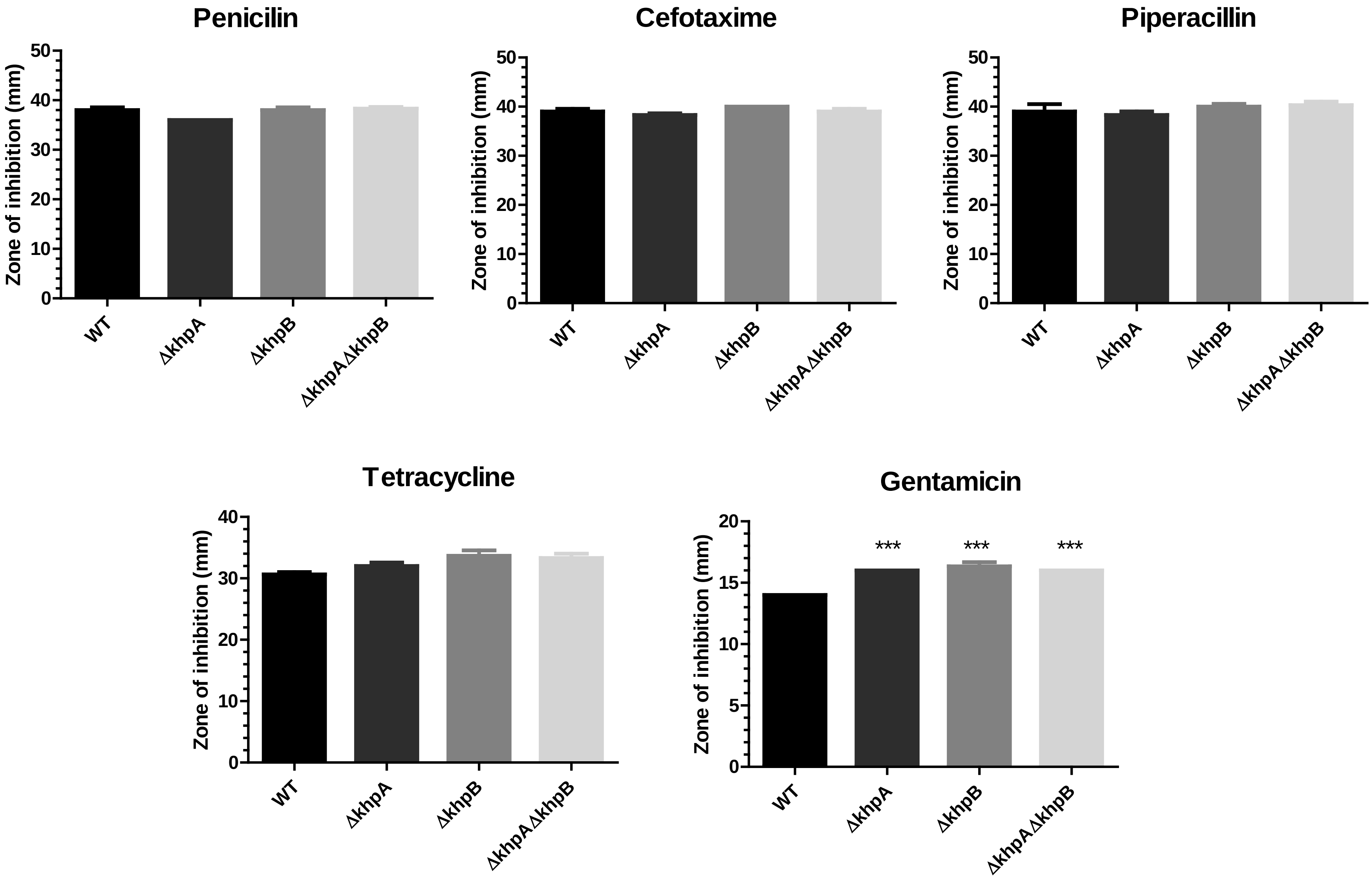
Penicilin
Cefotaxime
Piperacillin
Tetracycline
Gentamicin
Zone of inhibition (mm)
0
10
20
30
40
50
5
15
***
***
***
WT
ΔkhpA
ΔkhpB
ΔkhpAΔkhpB

Fig. S19

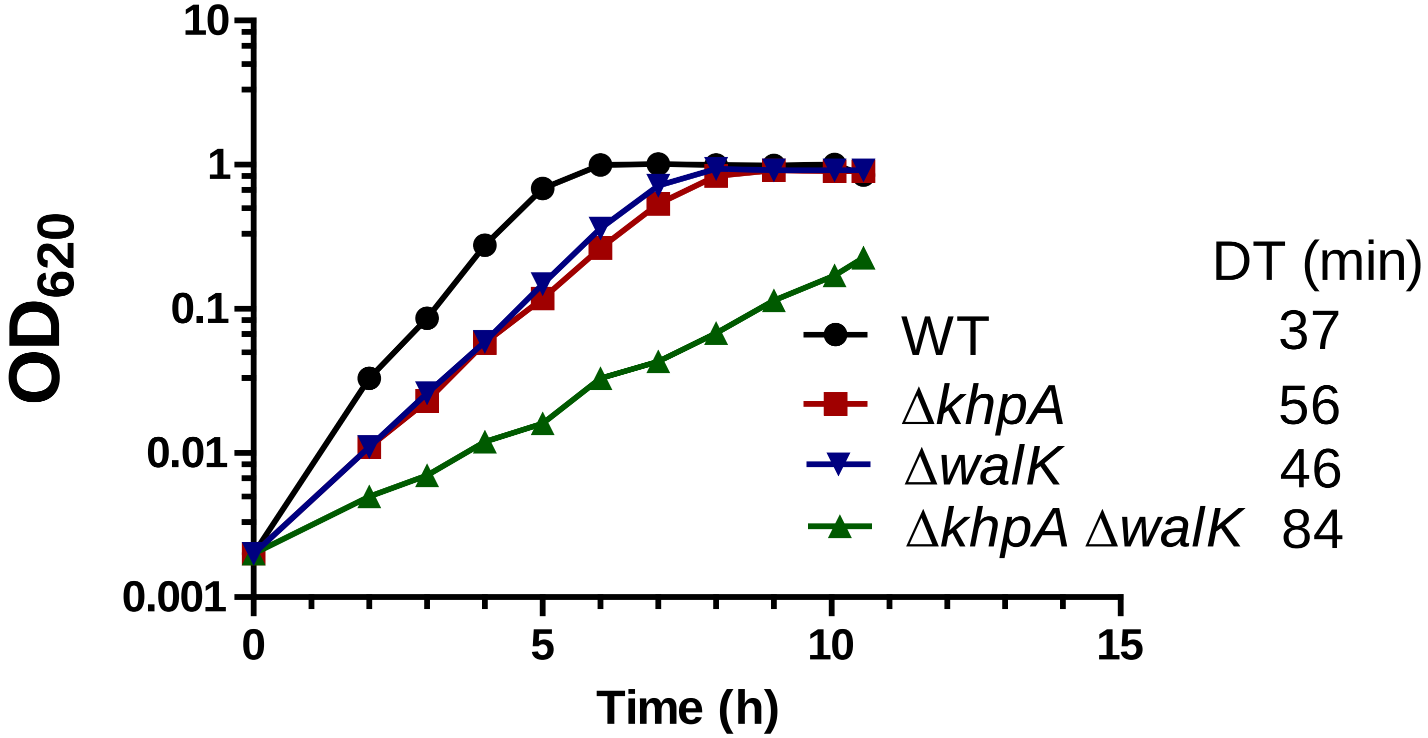
OD$_{620}$
10
1
0.1
0.01
0.001
0
5
10
15
Time (h)
DT (min)
WT 37
ΔkhpA 56
ΔwalK 46
ΔkhpA ΔwalK 84

Fig. S20

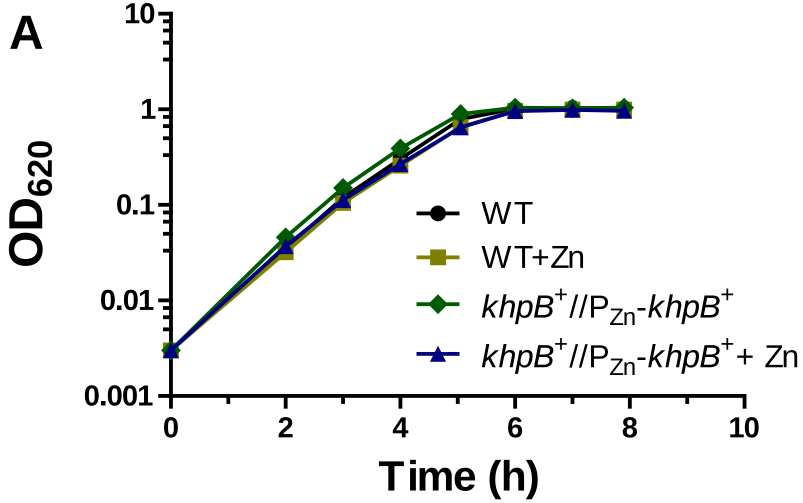

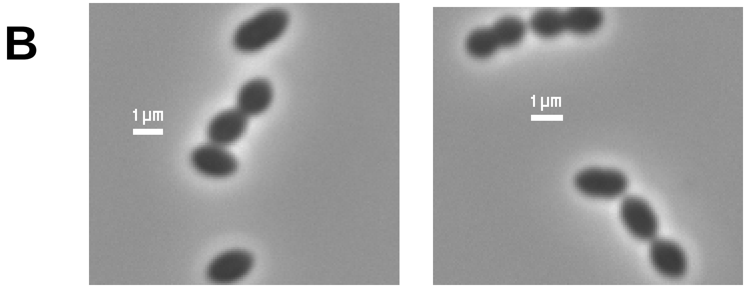

WT

WT + Zn

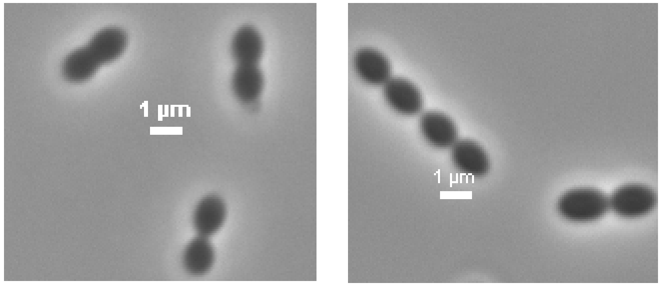

khpB$^+$//P_{Zn}-*khpB*$^+$

khpB$^+$//P_{Zn}-*khpB*$^+$ + Zn

Fig. S21

Table S4. RNAs pulled down by KhpA or KhpB in RIP-Seq experiments[a]

Table S4A. mRNAs and tRNAs pulled down by KhpA or KhpB [b,c,d]

Gene	***khpA* -L-F^3 to WT**		***khpB* -L-F^3 to WT**		**Description**
	log2Fold Ratio	**P-adjust**	**log2Fold Ratio**	**P-adjust**	
spd_0009	2.20	1.58E-30	1.93	1.63E-23	hypothetical protein
spd_0023	4.38	2.91E-32	3.96	1.95E-26	hypothetical protein (80 aa)
RS00670 (*spd_0124* and *spd_0125*)	2.45	2.09E-14	2.49	7.01E-15	hypothetical protein (65 aa)
spd_0138	2.11	1.78E-21	1.37	1.32E-09	glycosyl transferase
spd_0139	2.26	5.17E-20	1.40	3.14E-08	glycosyl transferase family 2
spd_0174	2.05	7.87E-46	1.78	1.89E-34	DUF-1129 domain protein
spd_0220	1.83	2.85E-25	2.07	7.66E-32	ACT superfamily protein (88 aa)
spd_0324 (cps2I)	2.11	7.83E-28	1.98	2.18E-24	glycosyl transferase family 1
spd_0325	2.49	5.16E-14	2.06	8.62E-10	MATE_like protein
spd_408	2.13	1.43E-30	2.48	5.82E-41	hypothetical protein
RS02245 (*spd_0422* and *spd_0423*)	2.16	9.76E-05	1.41	1.45E-02	hypothetical protein
spd_0449	1.96	2.24E-17	1.85	1.91E-15	hypothetical protein (45 aa)
spd_0452	0.53	1.41E-01	2.46	2.19E-14	integrase
spd_0594	2.64	5.43E-67	2.62	9.36E-66	DUF3165 domain membrane protein (84 aa)
spd_0603	2.51	2.56E-25	2.41	3.20E-23	S2P-M50 superfamily protein
spd_0604 (hemY)	2.40	5.83E-32	2.30	2.42E-29	heme biosynthesis protein HemY
spd_0612	2.21	1.53E-10	1.74	6.88E-07	hypothetical protein
spd_0613	2.59	4.42E-27	1.83	7.99E-14	hypothetical protein
spd_0679 (trmD)	3.25	5.45E-162	1.06	8.40E-18	tRNA (guanosine(37)-N1)-methyltransferase
spd_0680	2.69	3.25E-100	0.83	2.72E-10	NRDD superfamily protein (92 aa)
spd_0688	2.06	1.43E-25	2.76	4.63E-45	PRK10535 superfamily membrane protein
spd_0703	2.84	1.41E-37	3.21	8.89E-48	WalRK regulon membrane protein (85 aa)
spd_0754	2.28	2.84E-33	2.39	3.28E-36	DUF-2969 domain protein (76 aa)
spd_0785	2.26	2.32E-50	2.40	1.44E-56	hypothetical protein (66 aa)
RS04590 (*spd_0860* and *spd_0861*)	2.40	2.41E-24	2.14	1.82E-19	50S ribosomal protein L33
spd_0897	1.96	4.35E-12	1.31	7.82E-06	sugar translocase
RS04875 (*spd_0914* and *spd_0915*)	2.30	6.02E-25	2.22	3.04E-23	hypothetical protein (87 aa)
RS04880 (*spd_0914* and *spd_0915*)	2.37	7.38E-39	2.52	1.21E-43	transcriptional regulator (72 aa)
RS04905 (*spd_0918* and *spd_0919*)	2.59	1.44E-25	2.15	7.30E-18	methylase_S protein
spd_0919	2.38	2.41E-24	2.12	2.14E-19	DUF-4286 protein (51 aa)

spd_0932	2.99	1.51E-41	2.46	2.71E-28	PHP superfamily protein
spd_0933	2.54	3.39E-40	2.52	1.32E-39	ABC_ATPase protein
spd_0946	2.62	1.58E-10	2.43	4.01E-09	Class II_aaRS-like-core superfamily
spd_0947	2.03	7.57E-10	1.90	1.12E-08	hypothetical protein
spd_0963	3.66	6.42E-78	4.18	2.36E-101	DUF4044 domain membrane protein (44 aa)
spd_1003	2.99	1.16E-39	2.87	1.33E-36	hypothetical protein (67 aa)
RS05675 (spd_1069 and *spd_1070)*	2.40	4.31E-28	1.85	6.02E-17	hypothetical protein
spd_1071	2.56	4.18E-41	2.36	6.57E-35	SIR2 domain protein
spd_1159	3.69	4.48E-39	3.43	9.00E-34	hypothetical protein (56 aa)
spd_1164 (cdd2)	2.00	3.30E-12	1.35	5.35E-06	cytidine deaminase
spd_1165	3.24	4.77E-33	3.07	8.17E-30	phosphatidylglycerophosphatase A
spd_1177	2.31	3.85E-12	2.11	2.76E-10	multidrug ABC transporter ATP-binding protein
RS06640 (spd_1258 and *spd_1259)*	2.97	5.58E-52	2.95	5.32E-51	restriction endonuclease (60 aa)
spd_1260	2.16	1.36E-28	2.06	5.99E-26	site-specific DNA-methyltransferase
spd_1265	2.08	3.38E-09	1.65	4.29E-06	trep-strep superfamily membrane protein
spd_1315	2.31	3.75E-06	1.82	3.61E-04	pseudogene transposase
spd_1317	2.21	1.70E-19	2.01	4.46E-16	hypothetical protein (46 aa)
RS07625 (spd_1447 and *spd_1448)*	2.44	9.49E-24	2.39	1.17E-22	hypothetical protein (100 aa)
RS07695 (spd_1458 and *spd_1459)*	2.10	9.43E-23	2.12	3.89E-23	hypothetical protein
spd_1477 (sepF)	2.52	2.94E-48	1.74	2.20E-23	cell division protein SepF
spd_1587	2.17	6.23E-35	2.03	1.03E-30	aspartate aminotransferase
RS08415 (spd_1591 and *spd_1592)*	1.73	4.83E-15	1.98	1.98E-19	transposase
spd_1614	2.56	5.75E-10	2.01	1.97E-06	PhoU family transcriptional regulator
spd_1616	2.73	5.71E-14	2.75	4.17E-14	hypothetical protein (98 aa)
spd_1683 (*tRNA-Ile*)	2.49	1.24E-34	2.63	1.60E-38	tRNA-Ile
spd_1684 (*tRNA-Gly*)	1.90	9.55E-18	2.09	2.53E-21	tRNA-Gly
spd_1690 (*tRNA-Pro*)	2.49	6.20E-21	2.31	4.51E-18	tRNA-Pro
spd_1691 (*tRNA-Arg*)	2.53	3.70E-26	2.35	1.13E-22	tRNA-Arg, duplicate gene *spd_1805*
spd_1692 (*tRNA-Leu*)	2.00	9.49E-23	1.92	4.54E-21	tRNA-Leu, duplicate gene *spd_1806*
spd_1693 (*tRNA-Gly*)	2.63	9.33E-27	2.45	3.20E-23	tRNA-Gly, duplicate gene *spd_1807*
spd_1694 (*tRNA-Thr*)	4.22	1.86E-127	4.00	2.78E-114	tRNA-Thr, duplicate gene *spd_1808*
spd_1749	1.95	6.13E-15	1.77	2.79E-12	bacteriocin formation protein
spd_1756	2.12	1.01E-08	1.62	2.15E-05	hypothetical protein (63 aa)
RS09330 (spd_1764 and *spd_1765)*	2.59	2.06E-28	2.45	2.89E-25	DUF1146 superfamily protein
spd_1783	1.97	1.33E-29	1.78	4.64E-24	hypothetical protein
spd_1803	2.07	1.07E-35	1.60	1.28E-21	hypothetical protein (68 aa)
spd_1804	3.96	4.67E-51	4.18	1.44E-56	tRNA-Pro
spd_1805	2.53	3.70E-26	2.35	1.13E-22	tRNA-Arg, duplicate gene *spd_1691*

spd_1806	2.00	9.49E-23	1.92	4.54E-21	tRNA-Leu, duplicate gene *spd_1692*
spd_1807	2.63	9.33E-27	2.45	3.20E-23	tRNA-Gly, duplicate gene *spd_1693*
spd_1808	4.22	1.86E-127	4.00	2.78E-114	tRNA-Thr, duplicate gene *spd_1694*
spd_1828	2.36	1.11E-28	2.30	3.34E-27	ABC transporter ATP-binding protein
spd_1842 (*araD*)	0.21	5.33E-01	2.01	2.92E-14	L-ribulose-5-phosphate 4-epimerase
spd_1844 (*ulaD*)	0.93	6.25E-02	2.37	1.61E-07	3-keto-L-gulonate-6-phosphate decarboxylase
spd_1845	0.05	9.46E-01	2.27	3.04E-05	PTS ascorbate transporter subunit IIA
spd_1846	0.18	7.49E-01	2.36	1.49E-08	PTS ascorbate transporter subunit IIB
spd_1847	0.00	9.99E-01	2.43	5.98E-11	PTS ascorbate transporter subunit IIC
spd_1848	0.57	4.37E-04	4.25	4.01E-174	hypothetical protein
spd_1864	2.25	4.19E-23	2.80	3.96E-35	DUF-1033 superfamily protein
spd_1871	1.92	1.62E-12	2.04	7.10E-14	hypothetical protein (99 aa)
spd_1879 (*tRNA-Leu*)	2.16	1.42E-23	2.33	2.36E-27	tRNA-Leu
spd_1880 (*tRNA-Gln*)	1.86	1.92E-19	2.09	3.27E-24	tRNA-Gln
spd_1995 (*fucK*)	1.21	1.23E-05	2.26	3.49E-17	L-fuculose kinase
spd_2006 (*dltX*)	2.05	2.20E-09	2.40	1.91E-12	D-ala-teichoic acid biosynthesis protein DltX (43 aa)
spd_2066 (*tRNA-Arg*)	2.42	1.92E-24	2.65	7.45E-29	tRNA-Arg
spd_2067 (*rlmH*)	2.73	9.77E-31	2.94	1.39E-35	rRNA large subunit methyltransferase

Table S4B. Intergenic RNAs and sRNAs pulled down by KhpA or KhpB^{c,d,e}

D39 genome locus (bp)		***khpA* -L-F^3 to WT**		***khpB* -L-F^3 to WT**		**Nearest gene**	**Distance to nearest gene**	**Nearest gene description**
Start	**End**	**log2Fold Ratio**	**P-adjust**	**log2Fold Ratio**	**P-adjust**			
14901	15000	3.62	1.29E-38	3.51	4.43E-36	*spd_0015*	3	tRNA-Glu
15001	15100	3.68	9.62E-127	3.73	1.10E-129	*spd_0016*	50	16S ribosomal RNA
39901	40000	2.58	4.44E-08	2.33	1.21E-06	*spd_0047*	29	hypothetical protein
40101	40200	2.45	6.39E-12	2.21	1.08E-09	*spd_0048*	24	ISL3 family transposase
74401	74500	1.57	9.97E-03	2.17	2.17E-04	*spd_0073*	53	chlorohydrolase
119101	119200	2.06	1.10E-03	2.63	1.89E-05	*spd_0116*	170	hypothetical protein
120501	120600	1.86	1.88E-02	2.63	5.20E-04	*spd_0118*	222	hypothetical protein
120601	120700	1.97	1.80E-03	1.88	3.41E-03	*spd_0118*	322	hypothetical protein
120901	121000	2.10	3.97E-05	2.16	2.50E-05	*spd_0119*	84	hypothetical protein
126801	126900	2.62	2.86E-05	2.59	4.05E-05	*spd_0125*	7	hypothetical protein
142501	142600	2.15	3.12E-03	1.44	6.93E-02	*spd_0138*	4	glycosyl transferase
146401	146500	2.63	1.51E-05	1.98	2.00E-03	*spd_0140*	20	ABC transporter ATP-binding protein
146601	146700	2.51	1.47E-03	1.00	2.83E-01	*spd_0141*	30	hypothetical protein
170101	170200	2.82	1.34E-14	2.98	3.58E-16	*spd_0165*	80	DNA mismatch repair protein HexB
170201	170300	1.90	6.33E-14	2.23	7.31E-19	*spd_0166*	46	6,7-dimethyl-8-ribityllumazine synthase
173801	173900	3.62	1.49E-22	3.34	4.34E-19	*spd_0169*	42	bifunctional reductase
173901	174000	3.52	1.71E-21	3.80	7.64E-25	*spd_0169*	142	bifunctional reductase
233701	233800	1.99	2.58E-08	1.32	5.11E-04	*spd_0242*	21	hypothetical protein
233801	233900	2.57	3.51E-15	2.37	6.47E-13	*spd_0243*	11	isoprenyl transferase
257901	258000	2.14	1.32E-37	2.09	7.97E-36	*spd_0260*	91	16S rRNA pseudouridine(516) synthase
284301	284400	2.83	9.77E-09	2.78	2.29E-08	*spd_0285*	36	alpha-xylosidase
394501	394600	2.58	5.84E-22	1.85	1.76E-11	*spd_0391*	315	hypothetical protein
394701	394800	2.59	9.12E-14	1.82	4.71E-07	*spd_0393*	153	N utilization substance protein B homolog
423201	423300	2.38	1.22E-04	1.66	1.22E-02	*spd_0422*	38	hypothetical protein
423401	423500	2.09	7.62E-08	2.08	9.49E-08	*spd_0423*	55	hypothetical protein
457801	457900	1.96	2.17E-03	2.05	1.38E-03	*spd_0450*	85	hypothetical protein
503801	503900	3.08	1.10E-22	3.01	1.59E-21	*spd_0496*	8	cell division protein Fic
534701	534800	2.56	8.88E-04	2.25	4.34E-03	*spd_0524*	60	DNA-binding response regulator
565601	565700	1.92	1.91E-04	2.16	2.41E-05	*spd_0554*	419	ABC transporter ATP-binding protein
576501	576600	1.95	3.14E-03	2.38	2.53E-04	*spd_0558*	119	serine protease
576601	576700	2.03	2.64E-04	2.74	3.95E-07	*spd_0558*	219	serine protease
626601	626700	2.24	4.79E-07	2.16	1.56E-06	*spd_0600*	85	cell division protein DivIB

626901	627000	2.35	2.77E-22	2.46	2.74E-24	*spd_0603*	307	hypothetical protein
627001	627100	2.81	1.75E-09	2.80	2.54E-09	*spd_0603*	207	hypothetical protein
627101	627200	2.66	6.86E-11	2.53	7.65E-10	*spd_0603*	107	hypothetical protein
642001	642100	2.08	1.05E-03	1.86	4.41E-03	*spd_0620*	130	lysine--tRNA ligase
642101	642200	3.16	6.43E-06	2.46	7.49E-04	*spd_0620*	230	lysine--tRNA ligase
646801	646900	1.79	2.33E-06	2.55	5.06E-12	*spd_0625*	215	cobalt ABC transporter permease
646901	647000	2.98	1.66E-09	2.85	1.04E-08	*spd_0625*	115	cobalt ABC transporter permease
647001	647100	2.17	7.11E-05	1.63	4.72E-03	*spd_0625*	15	cobalt ABC transporter permease
685001	685100	3.09	1.79E-05	0.27	7.98E-01	*spd_0664*	161	S-adenosylmethionine synthase
694601	694700	3.22	2.38E-13	-0.33	6.32E-01	*spd_0675*	57	KhpA, RNA-binding protein
694701	694800	6.07	2.50E-39	0.21	7.96E-01	*spd_0675*	157	KhpA, RNA-binding protein
694801	694900	5.90	2.50E-50	0.46	4.38E-01	*spd_0676*	221	alpha/beta hydrolase
694901	695000	5.74	3.16E-36	0.20	7.97E-01	*spd_0676*	121	alpha/beta hydrolase
695001	695100	5.36	2.15E-18	0.49	5.99E-01	*spd_0676*	21	alpha/beta hydrolase
727601	727700	2.43	2.78E-07	2.09	1.72E-05	*spd_0712*	147	transposase
727701	727800	2.29	2.89E-05	1.84	1.25E-03	*spd_0712*	47	transposase
737901	738000	1.98	5.81E-03	2.03	4.98E-03	*spd_0722*	75	ADP-dep(S)-NAD(P)H-hydrate dehydratase
738001	738100	2.43	1.41E-04	2.11	1.34E-03	*spd_0723*	8	ribose-5-phosphate isomerase
799901	800000	3.22	4.50E-32	3.06	9.25E-29	*spd_0784*	69	DEAD/DEAH box helicase
800001	800100	2.98	1.30E-34	2.87	4.50E-32	*spd_0785*	3	hypothetical protein
809601	809700	1.76	1.76E-02	2.18	2.67E-03	*spd_0791*	78	chlorohydrolase
810801	810900	2.78	6.16E-06	2.44	1.02E-04	*spd_0792*	186	membrane protein
810901	811000	2.04	1.06E-03	2.09	8.54E-04	*spd_0792*	86	membrane protein
820301	820400	1.58	2.06E-03	2.38	9.06E-07	*spd_0803*	124	membrane protein
926501	926600	2.29	1.12E-06	2.04	2.30E-05	*spd_0914*	35	hypothetical protein
927401	927500	1.93	9.74E-10	2.17	4.59E-12	*spd_0915*	24	transcriptional regulator
927501	927600	2.38	4.38E-20	2.45	3.30E-21	*spd_0915*	124	transcriptional regulator
927601	927700	2.22	2.09E-03	2.35	1.15E-03	*spd_0915*	70	hypothetical protein
931601	931700	2.36	7.98E-10	1.71	2.20E-05	*spd_0918*	8	iron ABC transporter ATP-binding protein
931701	931800	2.31	3.57E-08	1.93	7.65E-06	*spd_0918*	108	iron ABC transporter ATP-binding protein
931801	931900	2.95	2.58E-06	2.77	1.33E-05	*spd_0918*	208	iron ABC transporter ATP-binding protein
932701	932800	4.44	6.68E-37	4.17	2.28E-32	*spd_0919*	51	hypothetical protein
932801	932900	2.24	9.49E-04	2.44	2.95E-04	*spd_0919*	151	hypothetical protein
933001	933100	2.21	2.99E-03	1.64	3.88E-02	*spd_0920*	234	hypothetical protein
942201	942300	2.57	1.79E-11	2.15	4.57E-08	*spd_0930*	114	transcriptional regulator
962501	962600	1.20	1.34E-01	1.97	8.14E-03	*spd_0951*	184	transcriptional regulator
1006701	1006800	3.24	8.86E-26	3.02	3.44E-22	*spd_0998*	99	ABC transporter ATP-binding protein
1028001	1028100	2.16	9.14E-18	2.15	1.76E-17	*spd_1013*	22	IS630 family transposase
1047201	1047300	2.89	1.04E-06	3.22	3.92E-08	*spd_1021*	176	ribonuclease HII
1047301	1047400	2.22	4.22E-04	1.96	2.45E-03	*spd_1023*	209	tyrosine recombinase XerS
1047401	1047500	2.66	1.68E-05	2.47	9.00E-05	*spd_1023*	109	tyrosine recombinase XerS

1074101	1074200	2.46	1.10E-04	2.08	1.61E-03	*spd_1044*	31	DeoR family transcriptional regulator
1174601	1174700	2.04	8.53E-13	2.11	1.83E-13	*spd_1041*	97	uracil transporter
1186601	1186700	1.97	1.80E-03	1.88	3.59E-03	*spd_1157*	286	transposase
1188701	1188800	4.35	7.17E-23	4.21	2.41E-21	*spd_1159*	45	hypothetical protein
1192301	1192400	2.07	3.38E-04	0.73	3.06E-01	*spd_1164*	64	cytidine deaminase
1207301	1207400	2.44	4.87E-04	2.55	2.78E-04	*spd_1178*	183	prolyl oligopeptidase
1231101	1231200	1.70	1.57E-11	2.06	1.76E-16	*spd_1202*	80	LytR family transcriptional regulator
1267401	1267500	3.24	2.28E-12	2.84	1.62E-09	*spd_1236*	43	regulatory protein Spx
1282101	1282200	2.50	4.17E-05	2.07	1.09E-03	*spd_1253*	75	transcriptional regulator
1282201	1282300	2.93	1.09E-05	2.59	1.47E-04	*spd_1254*	111	ABC transporter permease
1282301	1282400	2.77	1.14E-04	1.32	1.08E-01	*spd_1254*	11	ABC transporter permease
1283901	1284000	3.23	2.31E-07	3.52	1.32E-08	*spd_1255*	27	ABC transporter ATP-binding protein
1287501	1287600	2.35	9.99E-05	2.51	3.04E-05	*spd_1258*	6	restriction endonuclease
1287801	1287900	2.04	1.14E-11	2.25	5.08E-14	*spd_1258*	13	restriction endonuclease
1289401	1289500	2.00	4.30E-10	1.91	3.17E-09	*spd_1260*	63	site-specific DNA-methyltransferase
1289601	1289700	2.29	2.66E-04	2.05	1.46E-03	*spd_1262*	165	AraC family transcriptional regulator
1289701	1289800	2.90	5.45E-09	2.87	1.02E-08	*spd_1262*	65	AraC family transcriptional regulator
1357001	1357100	2.20	1.26E-03	1.33	7.78E-02	*spd_1342*	92	IS30 family transposase
1421801	1421900	2.07	6.50E-05	1.53	5.29E-03	*spd_1403*	142	1,4-beta-N-acetylmuramidase
1455601	1455700	1.98	3.33E-07	1.83	3.48E-06	*spd_1438*	72	cadmium resistance protein CadD
1468701	1468800	3.12	1.36E-10	3.25	1.98E-11	*spd_1455*	19	hypothetical protein
1548301	1548400	2.84	9.27E-08	2.93	3.85E-08	*spd_1526*	50	membrane protein
1548401	1548500	3.09	5.23E-26	2.95	1.08E-23	*spd_1526*	150	membrane protein
1586201	1586300	2.86	2.97E-10	2.52	5.63E-08	*spd_1568*	67	NADPH-dependent reductase QueF
1604201	1604300	1.71	3.65E-02	2.37	2.55E-03	*spd_1587*	20	aspartate aminotransferase
1619401	1619500	2.86	3.10E-29	2.18	6.86E-17	*spd_1605*	19	LacI family transcriptional regulator
1704801	1704900	5.05	3.50E-142	5.03	1.03E-140	*spd_1703*	62	tRNA-Glu
1730701	1730800	2.41	8.69E-09	2.10	8.94E-07	*spd_1738*	133	MATE family efflux transporter
1750701	1750800	2.40	1.79E-03	1.96	1.42E-02	*spd_1756*	9	hypothetical protein
1750901	1751000	2.24	8.10E-05	1.69	4.73E-03	*spd_1756*	209	hypothetical protein
1759401	1759500	2.77	3.56E-05	2.72	5.98E-05	*spd_1760*	80	tRNA-Cys
1792101	1792200	2.13	1.60E-06	2.06	3.90E-06	*spd_1798*	94	DNA-binding response regulator
1796001	1796100	3.85	1.82E-11	3.30	1.77E-08	*spd_1803*	2	hypothetical protein
1796101	1796200	1.95	1.57E-03	1.58	1.47E-02	*spd_1803*	102	hypothetical protein
1796201	1796300	2.16	2.25E-03	1.66	2.67E-02	*spd_1803*	202	hypothetical protein
1796301	1796400	4.86	1.18E-26	4.44	4.31E-22	*spd_1804*	187	tRNA-Pro
1796401	1796500	3.06	1.28E-19	2.59	4.31E-14	*spd_1804*	87	tRNA-Pro
1802301	1802400	3.04	2.51E-115	3.06	3.94E-117	*spd_1816*	40	16S ribosomal RNA
1802401	1802500	6.43	3.40E-126	6.49	1.65E-128	*spd_1817*	13	tRNA-Glu
1813201	1813300	1.99	8.09E-04	1.93	1.42E-03	*spd_1827*	126	C4-dicarboxylate ABC transporter
1813701	1813800	2.02	2.39E-03	2.22	7.76E-04	*spd_1828*	129	ABC transporter ATP-binding protein

1818701	1818800	3.44	1.36E-06	1.91	1.47E-02	*spd_1833*	380	PTS cellobiose transporter subunit IIA
1862401	1862500	5.12	4.12E-65	5.44	2.79E-73	*spd_1891*	9	23S ribosomal RNA
1864201	1864300	2.55	1.28E-54	2.57	1.49E-55	*spd_1893*	15	16S ribosomal RNA
1864301	1864400	5.36	8.93E-105	5.50	6.13E-110	*spd_1894*	38	tRNA-Glu
1902301	1902400	2.12	1.69E-09	2.50	7.41E-13	*spd_1931*	78	membrane protein
2006301	2006400	2.20	7.24E-08	3.71	4.63E-21	*spd_2027*	45	hypothetical protein
2046001	2046100	2.73	2.78E-04	1.76	3.07E-02	*spd_2069*	98	chromosome segregation protein

Intergenic region between ftsA and upstream gene *spd_1481* (1496852 to 1497071)

1496901	1497000	1.62	4.006E-02	1.19	1.614E-01	*spd_1480*	49	cell division protein FtsA

[a] RNA immunoprecipitation samples were prepared from three independent cultures of IU1945 (WT), IU9602 (*khpA* -L-F^3) and IU10664 (*khpB* -L-F^3) and sequencing (RIP-Seq) analyses were performed as described in Experimental procedures. Log2-fold ratios and P-adjust values are based on three independent biological replicates of IU9602 compared to IU1945 or IU10664 compared to IU1945. Complete RIP-Seq procedures and data are deposited in the GEO database (accession number GSE103735).

[b] mRNA and tRNA gene designations are based on the original published *Streptococcus pneumoniae* D39 sequences (https://www.ncbi.nlm.nih.gov/nuccore/116075884?report=genbank) and an updated annotation (https://www.ncbi.nlm.nih.gov/nuccore/116515308) that includes new gene designations prefixed with SPD_RS. SPD_RS genes that do not have corresponding spd numbers are followed by the two adjacent spd genes in parenthesis. Ratios of reads are obtained with reads covering the whole gene. Some RNAs show a log2ratio > 2 in one segment of the gene, but do not show an overall log2fold ratio of >2 in this analysis.

[c] Both tables S4A and S4B contain only mRNA, tRNA or 100-bp segments of intergenic regions with a log2-fold value > 2 and an P-adjust value<0.01 for both IU9602 compared to IU1945, and IU10664 compared to IU1945.

[d] RNA or intergenic regions highlighted in yellow or orange show log2Fold ratio >2 and P-adjust values < 0.01 in the comparison of *khpA* -L-F^3 vs WT , but show log2Fold ratio <1 and P-adjust values > 0.01 in the comparison of *khpB* -L-F^3 vs WT, or vice versa. Regions highlighted in yellow represent genes downstream of *khpB* , or the intergenic region downstream of *khpA* . These increases are due to the inserted promoter of Pc-erm of the *khp* A-L-F^3 or *khpB* -L-F^3 strains.

[e] Intergenic regions highlighted in green overlapped with previous identified sRNA Spd-sr7 (820183 to 820245) or Spd-sr10 (1750985 to 1751149) (Tsui, H.C., D. Mukherjee, V.A. Ray, L.T. Sham, A.L. Feig & M.E. Winkler, (2010) Identification and characterization of noncoding small RNAs in *Streptococcus pneumoniae* serotype 2 strain D39. Journal of bacteriology 192: 264-279.)